Atmospheric wet and dry deposition of trace elements at ten sites in Northern China

Y. P. Pan and Y. S. Wang

State Key Laboratory of Atmospheric Boundary Layer Physics and Atmospheric Chemistry (LAPC), Institute of Atmospheric Physics, Chinese Academy of Sciences, Beijing 100029, China

Correspondence to: Y. S. Wang (*wys@mail.iap.ac.cn; panyuepeng@mail.iap.ac.cn*)

Abstract

Atmospheric deposition is considered to be a major process that removes pollutants from the atmosphere and an important source of nutrients and contaminants for ecosystems. Trace elements (TEs), especially toxic metals deposited on plants and into soil or water, can cause substantial damage to the environment and human health due to their transfer and accumulation in food chains. Despite public concerns, quantitative knowledge of metal deposition from the atmosphere to ecosystems remains scarce. To advance our understanding of the spatio-temporal variations in the magnitudes, pathways, compositions and impacts of atmospherically deposited TEs, precipitation (rain and snow) and dry-deposited particles were collected simultaneously at ten sites in Northern China from December 2007 to November 2010.

The measurements showed that the wet and dry depositions of TEs in the target areas were orders of magnitude higher than previous observations within and outside China, generating great concern over the potential risks. The spatial distribution of the total (wet plus dry) deposition flux was consistent with that of the dry deposition, with a significant decrease from industrial and urban areas to suburban, agricultural and rural sites, while the wet deposition exhibited less spatial variation. In addition, the seasonal variation of wet deposition was also different from that of dry deposition, although they were both governed by the precipitation and emission patterns.

For the majority of TEs that exist as coarse particles, dry deposition dominated the total flux at each site. This was not the case for potassium, nickel, arsenic, lead, zinc, cadmium, selenium, silver and thallium, for which the relative importance between wet and dry deposition fluxes varied by site. Whether wet deposition is the major atmospheric cleansing mechanism for the TEs depends on the size distribution of the particles.

We found that atmospheric inputs of copper, lead, zinc, cadmium, arsenic and selenium were of the same magnitude as their increases in the topsoil of agricultural

systems. At a background forest site in Northern China, the total deposition flux of lead observed in this study (14.1 mg m^{-2} yr^{-1}) was twice that of the critical load calculated for temperate forest ecosystems in Europe. These findings provide baseline data needed for future targeting policies to protect various ecosystems from long-term heavy metal input via atmospheric deposition.

1 Introduction

Air pollution is generally considered an accumulation in the atmosphere of substances that, in sufficient concentrations resulting from excessive anthropogenic emissions and natural sources, endanger human health and the environment. In recent decades, public concern regarding the consequences of worldwide air pollution has motivated considerable political debate regarding emissions control (Chen et al., 2014). In addition to mitigation measures taken by local governments, two primary natural processes have been recognized as participating in the reduction of air pollutants: dry and wet deposition. The removal of pollutants from the atmosphere by wet deposition is often considered an important natural mediating factor in cleansing the atmosphere (Yang et al., 2012). In an eastern U.S. deciduous forest, for example, wet deposition rates for single events were several orders of magnitude greater than dry deposition rates measured for periods between precipitation events (Lindberg and Harriss, 1981). In contrast to the episodic nature of wet deposition, however, dry deposition is a continuous and dependable process involved in atmospheric cleansing (Grantz et al., 2003). In regions with low precipitation, such as Mediterranean climate area (Muezzinoglu and Cizmecioglu, 2006), dry deposition as a cleansing mechanism is more important than wet deposition on an annual basis. Thus, the relative importance of wet versus dry deposition may depend on the efficiencies of these two mechanisms, but it also varies with the local availability of precipitation (Muezzinoglu and Cizmecioglu, 2006). In the absence of simultaneous measurements of these two processes, however, their relative and combined contributions to the total deposition remain unclear, and debate remains over whether dry deposition is the major cleansing mechanism.

Although natural deposition cleans the atmosphere, its ultimate result is the transfer of nutrients (e.g., reactive nitrogen species) and contaminants (e.g., heavy metals) from air into water and soil (Duan et al., 2010; Hovmand et al., 2008). In regions where natural biogeochemical cycles are perturbed by human activities, atmospheric deposition can be important sources of either toxic substances or nutrients for the ecosystems (Hovmand et al., 2009; Meng et al., 2008). Thus, the interest in atmospheric deposition results mostly from concerns regarding the effects of the deposited materials entering the terrestrial and aquatic environments as well as their subsequent health effects (Sakata et al., 2006). When estimating atmospheric deposition flux, it is also important to consider the global biogeochemical cycle. For example, when compared with the riverine input, atmospheric dry deposition is one of the major paths for the transport of chemical species from the continents to coastal and open marine ecosystems (Duce et al., 1991). On the regional scale, the dry deposition process may be particularly important near urban/industrial areas where particle concentrations and sizes are large, such as sites near the Great Lakes (Sweet et al., 1998). Compared with developed regions in the U.S. and Europe, however, relatively little is known about the magnitude and potential impacts of atmospheric deposition in the vast areas of Asia.

Northern China is subject to large quantities of emissions. However, measuring the atmospheric deposition flux, particularly the dry deposition of aerosols and their precursors, has thus far received little attention. The components of aerosols in Northern China are characterized by high levels of crustal elements (e.g., aluminum-Al, silicon-Si, iron-Fe, potassium-K, sodium-Na, barium-Ba and calcium-Ca) that are mainly generated over upstream arid/semi-arid areas (specifically, episodic dust storms in the springtime); the aerosols also contain abundant acids and heavy metals (e.g., copper-Cu, lead-Pb, zinc-Zn, cadmium-Cd, nickel-Ni, chromium-Cr, selenium-Se, vanadium-V, antimony-Sb and thallium-Tl) that are emitted directly from local anthropogenic sources (e.g., power plants, motor vehicles and industrial facilities) (Chen et al., 2014; Zhao et al., 2013). In addition to the complex emissions, the topography (surrounded by mountains) and climate (lack of rain) are not favorable for the diffusion and wet deposition of pollutants (e.g., sulfur dioxide, nitrogen dioxide and ammonia) in Northern China (Yang et al., 2012). Although previous studies have defined the aerosol/precipitation chemistry at a number of sites in the target areas, spatial and temporal information regarding wet and dry deposition derived from local and regional emissions in this complex air shed is limited. To advance our understanding of the transportation and transformation of pollutants from the local to the regional and global scales, our knowledge of the quantitative aspects of atmospheric deposition must be updated with detailed spatio-temporal descriptions. Therefore, a new monitoring network including ten well-distributed sites within the target areas was established in late 2007. The focus of the program was to evaluate the wet and dry deposition of the important trace species, including carbon, nitrogen, sulfur, phosphorus, heavy metals, and polycyclic aromatic hydrocarbons (PAHs). The observations of this monitoring network have recently been presented, with an emphasis on acids and nutrients that most affect natural ecosystems (Pan et al., 2012, 2013b; Pan et al., 2010a; Wang et al., 2012). With the substantial anthropogenic emissions, toxic metals deposited into ecosystems have led to increasing public concerns due to their transfer and accumulation in food chains (Luo et al., 2009).

In this paper, we further investigate the atmospheric wet and dry deposition fluxes of 25 trace elements (TEs) to complement the previous studies. The measurements were conducted during a three-year observation campaign at 10 selected sites. This study is the first attempt to conduct long-term direct measurements of the atmospheric deposition flux of crustal and anthropogenic metals in such a vast geographical area of China. The objectives of this research were (i) to clarify the spatial and seasonal variations in the wet and dry deposition fluxes across Northern China, (ii) to examine the relative importance of wet and dry deposition in removing airborne metals, and (iii) to compare the atmospheric deposition flux of TEs to other measurements in the literature and to the anthropogenic metal input to various ecosystems.

2 Materials and methods

2.1 Site description

Ten sites representing a range of conditions (coast-inland, forest-cropland, source-receptor, urban-rural, etc.) encountered in Northern China were selected for this study (Fig. 1). The observations of atmospheric deposition at all of the monitoring stations were conducted from December 2007 to November 2010. The monitoring network was operated and managed by the Institute of Atmospheric Physics, Chinese Academy of Sciences. The 10 sites are abbreviated using the names of the town/county/city in which they are located, and they are organized according to their urban geographies, energy structures and ecosystem types (Table 1). The types include urban (Beijing-BJ and Tianjin-TJ), industrial (Baoding-BD, Tanggu-TG and Tangshan-TS), suburban (Yangfang-YF and Cangzhou-CZ), agricultural (Yucheng-YC and Luancheng-LC) and rural (Xinglong-XL). The longitudes ranged from 114.69°E to 118.20°E, and latitudes ranged from 36.85°N to 40.38°N. The mean annual precipitation ranged from 400 to 800 mm, and mean annual air temperature was 8–14 °C; more detailed descriptions of the ten selected sites in the study have been reported elsewhere (Pan et al., 2012, 2013b).

2.2 Sampling and analysis

2.2.1 Wet and dry deposition sampler

In this study, wet-only rainwater and dry-deposited particles were collected using a custom wet-dry automatic sampler (APS-2B, Changsha Xianglan Scientific Instruments Co., Ltd., China). The sampler has been successfully used to collect wet deposition of various species but scarcely used for dry deposition in most of the previous studies (Huang et al., 2010; Wang et al., 2010; Wang et al., 2014; Zhang et al., 2011). Based on the automatic sampler we developed a unique technique sampling dry deposition using polyurethane foam (PUF)-filter combined with a glass bucket (detailed in Sect. 2.3.2). The wet-dry sampler was equipped with a 707 cm^2 aperture and a 177 cm^2 PUF-based glass bucket in separate containers to sample daily rainfall and monthly particulate dry deposition, respectively. Because the rainwater sensor allows the collection funnel of the cover device to open/close automatically when rainfall begins/ceases, wet and dry deposition can be collected separately with minor mixing between the two. The automatic wet-dry collector (height, 1.5 m) was installed on the ground if the underlying surface of the site was grass or lawn. When the underlying surface was bared soil or the site was next to concrete road, the sampler was positioned on the rooftop of a building approximately 5-14 m above ground (varied by site, Table 1), to avoid collecting local emissions such as re-suspended particles. A schematic of the sampler used is shown in Fig. S1. In addition, snow samples were collected as soon as possible after the snowfall events using a separate clean plastic bucket with an inner diameter of 22 cm. A detailed description of the sampling equipment and procedures is published elsewhere in a series of data reports (Pan et al., 2012, 2013b).

2.2.2 Sampling and treatment procedures for precipitation

The rainwater and melted snow samples were stored in a 50 mL polyethylene terephthalate (PET) bottle and frozen in a refrigerator at −20 °C immediately after collection at each site. The samples were then delivered in iceboxes to analytical laboratories in the State Key Laboratory of Atmospheric Boundary Layer Physics and Atmospheric Chemistry (LAPC, Beijing) by routine monthly site-maintenance visits. In the laboratory, a 20 mL of the precipitation (rainwater and snow) samples were acidified to pH~1 with 0.2 mL concentrated nitric acid (HNO_3, 65%, Merck, Germany) to dissolve the TEs associated with suspended particles and to prevent their adsorption on the walls of the bottle. The preserved samples were sealed from the atmosphere and stored in the dark at 4 °C until analysis, which was normally conducted within one month. All delivery and sample-handling processes were conducted using gloves to avoid pollution.

To ensure the quality of the sampling and to check for possible contaminants, two separate clean plastic bags overlapped in a bucket with an inner diameter of 15 cm have been used to collect precipitation at the initial stage of the experiment at the BJ and CZ sites during the site-maintenance visits. After the rainfall ceases the inner plastic bag containing rainwater was collected. Then the rainwater was acidified to pH~1 and analyzed. The results concurrently collected by the plastic bag and the automatic sampler showed no significant differences (Fig. S2 for selected TEs), indicating that the methodology used in the study was reliable and repeatable.

2.2.3 Sampling and treatment procedures for dry deposition

Dry-deposited airborne particles were collected using a PUF-based surrogate surface. Details of the sample preparation have been described previously (Pan et al., 2012, 2013b), but are repeated here for the reader's convenience. Briefly, a PUF filter (15 cm diameter and 1.35 cm thickness with a density of 0.021 g cm^{-3}) serving as the surrogate surface was placed in a glass bucket (15 cm inner diameter and 30 cm depth) to collect the dry-deposited particulate matter. At the end of each month, the PUF filter was replaced with a new one. For the first three months of the study, field blanks were handled identically to the samples at each site but were placed in the glass bucket for only 5 minutes. Subsequently, blank filters were taken once per filter change (i.e., monthly) at only the BJ site; the bucket was capped during the sampling period. Filters were handled to minimize contamination. After collection, the PUF filters were sealed in aluminum foil and frozen in a refrigerator at each site until delivery in clean iceboxes to LAPC by routine monthly site-maintenance visits.

To determine the metal content of the dry-deposited particles, the PUF filters were digested using a closed-vessel microwave digestion system (MARS 5, CEM Corporation, Matthews, NC, USA). The microwave oven could accommodate the simultaneous digestion of up to 40 Teflon vessels. Prior to use, the vessels were sonicated for 15 min with 10% HNO_3 and soaked in 2% HNO_3 overnight to prevent contamination. Finally, these vessels were rinsed with ultrapure water at least three times. Preliminary studies were conducted to determine the recoveries of TEs with various amounts of HNO_3 (65%, Merck, Germany), hydrogen peroxide (H_2O_2, 30%, Beijing Institute of Chemical Reagents, China) and hydrofluoric acid (HF, 40%, Merck, Germany). The results showed that the optimal combination was 5 mL of concentrated HNO_3, 2 mL H_2O_2 and 0.2 mL HF (Pan et al., 2010b). The filter was cut into ten to twenty equal portions to obtain a sample mass below 0.5 g, which is the working limit of the microwave vessels. This procedure also allowed for a comparison of the analysis results from multiple strips per filter. To ensure analytic quality, certified soil (GBW07401) and fly ash (GBW08401) materials were employed. Approximately 10 mg of these reference materials was accurately weighed and placed into a Teflon vessel along with the HNO_3, H_2O_2 and HF. Subsequently, the vessels were capped, fastened on the rack and placed in the microwave oven to undergo the digestion procedure; the temperature-controlled digestion procedure is illustrated in Fig. S3. After cooling to room temperature, the digests were carefully transported to PET vials and diluted with Milli-Q water to a final volume of 50 mL. All samples were stored in the dark at 4 °C prior to analysis. All observed results were blank corrected.

2.2.4 Trace metal analysis for wet and dry deposition

A multi-element analytical program was run at LAPC using an Agilent 7500a inductively coupled plasma mass spectrometry (ICP-MS, Agilent Technologies, Tokyo, Japan). The instrument was optimized daily in terms of sensitivity (Li (lithium), Y (yttrium), and Tl), level of oxide (Ce-cerium) and doubly charged ion (Ce) using a tuning solution containing 10 μg L^{-1} of Li, Y, Tl, Ce, and cobalt (Co) in 2% HNO_3. The standard optimization procedures and criteria specified in the manufacturer's manual were followed. The concentrations of 25 TEs were determined by ICP-MS after calibration using external standards (Agilent Technologies, Environmental Calibration Standard, Part# 5183-4688) and internal standards (^{45}Sc (scandium), ^{73}Gd (gadolinium), ^{115}In (indium) and ^{209}Bi (bismuth) at 20 μg L^{-1} in 2% HNO_3) added online during TEs analysis. The multi-element standard stock solution containing 10 or 1000 mg L^{-1} of TEs in nitric acid was diluted in 2% HNO_3 to obtain five calibration standards (1, 5, 10, 20 and 50 μg L^{-1} for Cu, Pb, Zn, Cd, Arsenic (As), beryllium (Be), Al, Mn, Ba, Co, Ni, Cr, Se, V, molybdenum (Mo), silver (Ag), Sb, Tl, thorium (Th) and uranium (U); 100, 500, 1000, 2000 and 5000 μg L^{-1} for Fe, K, Na, Ca and magnesium (Mg)) plus a blank that covered the expected range for the samples. The analytical reproducibility of the extract concentrations was assessed by replication (the same sample was analyzed three times). The relative percent differences for replicate samples were less than 5%. A check standard was analyzed after the initial calibration and again after every 12 samples. If the relative difference between the measured and actual concentrations was not within 10%, the instrument was recalibrated and the previous 12 samples were re-analyzed.

As noted above, two certified materials were prepared in parallel to ensure the quality of the obtained results. The recoveries of the target elements ranged between 78% and 115% with the exception of Al (75%). In all experiments, reagent blanks were measured separately. The filter blanks and the final concentrations of metals in the samples are reported after the field blank correction. The detection limits were better than 10 ng L^{-1} for most of the metals determined through analyses of blank samples. The average metal concentrations in the field blanks were well below the detection limits, indicating that no significant contamination occurred during the sampling, handling, delivery or measurement steps.

2.2.5 Statistics

The monthly wet deposition fluxes of TEs (${}_{wdf}$TEs) were obtained by multiplying the volume-weighted concentrations of TEs in the precipitation and the volume of precipitation measured by a standard rain gauge at each site during the sampling period. The monthly dry deposition fluxes of TEs (${}_{ddf}$TEs) were calculated by dividing the amount of TEs loaded on the PUF-filter by the surrogate surface area during the corresponding period. One-way analysis of variance (ANOVA) and nonparametric tests were conducted to examine the significance of the differences in the annual ${}_{wdf}$TEs and ${}_{ddf}$TEs for all ten sites. All analyses were conducted using the software SPSS 11.5 (SPSS Inc., Chicago, IL, USA) and Origin 8.0 (Origin Lab Corporation, Northampton, MA, USA). Statistically significant differences were defined as $P < 0.05$ unless otherwise stated.

2.3 Methodology evaluation and Uncertainty analysis

2.3.1 Acid digestion of precipitation samples

The HNO_3 digestion technique is a powerful tool for studying the acid soluble fraction and minimizing adsorption losses of metals and has therefore been used, in most of the previous studies (Cizmecioglu and Muezzinoglu, 2008; Heal et al., 2005), to determine the concentrations in rain samples. However, so far, the aspect of metal fractions/species in precipitation has not been thoroughly investigated and thus requires attention. To test if the HNO_3 concentration (1%) in the final samples was enough or not to dissolve the trace elements associated with suspended particles, especially for the crustal elements such as Al and Fe, elemental contents in different fractions for precipitation were further investigated by three experiments below. The procedures were applied to a series of 10 sequential rainwater samples collected on September 16, 2010 in Beijing to extract water-soluble (experiment a), acid-soluble (experiment b) and total metal concentrations (experiment c).

Experiment a: The first set of 10 mL precipitation samples were filtered through a 0.45 μm Sartorius membrane filter to remove the suspended particles, then the filtrate was acidified to pH~1 by 0.1 mL HNO_3. Thus, the determined metal concentrations in this set represent the water-soluble fraction

Experiment b: The second set of 10 mL unfiltered precipitation samples were acidified to pH~1 using 0.1 mL HNO_3 to extract acid-leachable fractions, the concentration of which was considered to represent the environmentally mobile material, termed the acid-soluble fraction.

Experiment c: The third set of 5 mL unfiltered precipitation samples were acid digested for determination of total metal content, with procedure similar to that of PUF filter samplers described in Sect.3.2. In the digestion of precipitation samples, an optimized sequential acid treatment with a mixture of 2 mL HNO_3, 1 mL H_2O_2 and 0.2 mL HF has been used. Digested samples were diluted to 10 mL volume by Milli-Q water and then transferred into PET bottles until analysis.

The results of the analysis showed that the mean concentrations of acid-soluble Na, Mg, K, Ca, Mn, Zn, As, Se, Mo, Cd, Sb, Tl and Th were comparable to that of the water-soluble fraction (Fig. 2), but somewhat lower than their total content with insignificant difference. The findings indicated that on one hand these TEs were well dissolved in the rainwater and the suspended insoluble particles were negligible, on the other hand the 1% HNO_3 was enough to dissolve these metals completely and to minimize adsorption losses. In contrast, the concentrations of acid-soluble Be, V, Co, Ni, Cu, Ba, U, Cr, Fe, Ag, Pb and Al were significantly higher than that of water-soluble fraction and lower than that of total metal content (Fig. 2), in particular for the latter five metals. It suggested that these metals, associated with substantial insoluble suspended particles in the rainwater, cannot be completely dissolved with 1% HNO_3 method. Thus, the method used in this study underestimated the total concentrations of crustal TEs, and hence their wet deposition flux.

2.3.2 Development of a new method estimating dry deposition

Compared to the case for wet deposition, many uncertainties exist in the methods of direct measurements and modeled estimates used to quantify dry deposition. To date, there is no commonly accepted technique that can be used to evaluate the accuracy of these methods. For direct measurements, various surrogate surfaces, mainly solid surfaces such as Teflon plates, filters and buckets, have been used in an attempt to quantify dry deposition. It was shown that both the collector geometry and the surface characteristics had a large impact on the amount of collected material (Dasch, 1985; Shannigrahi et al., 2005). Thus, we developed a uniform monitoring protocol based on a PUF-based glass bucket, with reasons below.

In general, a bucket can collect more dry-deposited material than Teflon, foil or coated foil surfaces, as suggested by Dasch (1985). In addition to the deposition fluxes of particulate matter, chemical species like PAHs measured by the bucket method were also higher than those by the plate for downward flux methods (Shannigrahi et al., 2005). The difference can be attributed to the geometry of the collector that affects the amount of material collected (Noll et al., 1988). Specifically, the bucket has a disturbed flow at the top and the flow around the plate is relatively undisturbed (or laminar) (Shannigrahi et al., 2005). As a result, the bucket collects more deposited material.

However, the dry deposited particles in the buckets could be re-suspended due to winds in dry season. To address this problem, additional materials such as marbles and glycerol can be used to stabilize the deposited dust (McTainsh et al., 1997). However, such treatments would make the subsequent sample collection and chemical analysis difficult, especially when the samples were contaminated with bird droppings, dead insects, etc. Although water (Sakata and Marumoto, 2004) or a greased and smooth surrogate surface (Yi et al., 2001b) has been successfully used to measure particulate dry deposition fluxes of organic and inorganic air pollutants in recent years, there is still no surface being established as a standard. Most of important, previously reported methods were time consuming and difficult to be used by an untrained operator in the field. There is an obvious incentive for developing a simple and cost-effective sampler capable of trapping airborne particles.

Besides the collector geometry, the surface characteristics have a large impact on the amount of collected material. It was shown by Dasch (1985) that a bucket collected less dry-deposited material than a water surface or a filter of nylon, quartz-fiber, or glass-fiber. Deposition appeared to be strongly influenced by the surface affinity for gases, but for particles high retention is one of the ideal characteristics. PUF, a popular sampling medium for gaseous persistent organic pollutants (POPs) (Chaemfa et al., 2009a; Harner et al., 2004), can also trap particulate POPs because of its high retention (Shoeib and Harner, 2002). On this line of thinking, it may be desirable to use PUF as the potential surface to collect particles, which is also very easy to make, handle and deploy.

To integrate the advantages of collector geometry and the surface characteristics mentioned above, the PUF-based bucket was designed in our study to collect dry deposition. This technique was evaluated and compared to the standard method recommended by the Ministry of Environmental Protection of China, which uses buckets containing glycol as an alternative surrogate. These two types of surface surrogates, i.e., glycol vs. PUF, were placed concurrently in separate buckets so that the comparison can be made. As shown in Fig. S4, the results observed for the two surfaces agreed well with each other, indicating that the PUF has a high efficiency in trapping dry-deposited particles, which is comparable with that of glycol surface. As an evidence, a more recent study also suggested that particles were trapped on the surface and within the body of the PUF disk, and fine (<1 μm) particles can form clusters of larger size inside the foam matrix (Chaemfa et al., 2009b).

In addition to the important features described above, the PUF surrogate surface can also prevent particle bounce and is relatively inexpensive. It can be used at a variety of locations and over various time intervals to delineate spatial and temporal information. After collection, it was divided into several pieces so that replicates would be easily processed. Finally, the PUF was considered to be applicable to the buckets to measure the deposition fluxes in the study, as a uniform monitoring protocol for the observation network in Northern China.

2.3.3 Uncertainty of dry deposition

Despite the advantages of PUF-based bucket method, uncertainties and problems also exist in this dry deposition sampling. For example, the impaction and interception of fine particles are important for vegetative canopies and their effects are not reproduced in the design of this method, and also any other standardized artificial collection device (Wesely and Hicks, 2000). As discussed by Shannigrahi et al. (2005), the bucket method may overestimate because it substantially suppresses the upward flux. Due to the gravitational settling, the upward flux of large particles representing mass is negligibly small compared with the downward flux. Thus, the deposition fluxes of particulate matter measured by bucket would be close to the net flux (downward minus upward) near urban/industrial areas where particle sizes are large. In regions with fine particles, however, dry deposition flux measured by the bucket may be higher than the net flux. Even though, sedimentation is considered to be the major mechanism of dry deposition for particles, even for heavy metal species primarily on small particles (Dasch, 1985), so that the PUF-based bucket method provides a gross understanding of atmospheric deposition.

The bucket method has also been criticized that the high container walls may restrict the entry of all but the largest particles deposited by gravitational settling, which would result in the underestimation of dry deposition. But Dasch (1985) found that deposition was similar to buckets with 25 cm high walls compared to buckets with only l cm walls, indicating a minor influence of the walls on particle deposition. Additional underestimation of dry deposition flux may be due to the adsorption of particles on the bucket inner wall, which is missed by the PUF filter at the bottom. But after the particles on the walls were rinsed with water, then dried and weighted, this part was found to be insignificant compared with that captured by the PUF filter. But if the conditions favor the adsorption such as the presence of dew or the humid weather keeping the bucket wet for a long time, further investigation is needed to address the degree to which particulate material is trapped on the bucket sides.

As indicated by Dasch (1985), the collector geometry is less important than the surface characteristics in controlling dry deposition, and the difference in particle collection appeared to be dominated by the retention of the surface. Although PUF filter has a high retention for particles with wide size (Chaemfa et al., 2009b), part of uncertainties link to the decomposition of PUF filter itself under high temperature during the long exposure period in summer. The decomposition of PUF filter will result in underestimation of the mass of dry deposition but it can be corrected with the concurrent sampling (i.e., another glass bucket was sealed during sampling to prevent the PUF filter from dry deposition). In addition, there are problems related to the volatilization of some reactive species during the relatively long sampling period (Pan et al., 2012), but this is not the case for the trace metals, most of which are stable in particles under ambient temperature.

Although the present approach is far from clearing up all the aspects of dry deposition, it adds substantially to the knowledge of atmospheric metal deposition in Northern China. Most importantly, the direct measurement is essential for model validation in the estimates of dry deposition. Our measurements are most likely to underestimate dry-deposited particles for the above reasons, but the estimates are not far from the real ones because the PUF filter is an efficient collection surface. This simple method has the potential to be a routine procedure for obtaining information on temporal and geographical distribution of dry deposition.

2.4 Supporting sampling and analysis

2.4.1 Size resolved aerosols

Elemental characterization of size-segregated particulate matter was performed synchronously at five sites including urban (BJ and TJ), industrial (BD and TS) and rural (XL) with bi-weekly resolution during the campaign between September 2009 and August 2010. At each site a cascade impactor operating at 28.3 L min^{-1} (Anderson Series 20-800, USA) was installed to collect aerosol samples in nine size ranges (<0.43, 0.43–0.65, 0.65–1.1, 1.1–2.1, 2.1–3.3, 3.3–4.7, 4.7–5.8, 5.8–9.0 and >9 μm). The sampling interval was 24 h at the BJ, TJ, BD and TS sites, but for 48 h at the XL site to collect enough particles permitting a complete chemical analysis. The collected samples were digested with procedures similar to that of PUF filter and then analyzed by ICP/MS (see Sect. 2.2, for detailed analysis methods).

2.4.2 Soil profile

There were no soil parameter observations for the ten monitoring sites in this study; the soil profile elemental data presented were obtained from the Chinese Ecosystem Research Network available on the Data Sharing System website (http://www.cerndata.ac.cn/). Soil profile samples at two agricultural sites of LC, YC and one forest site near BJ were collected in September 2005, in compliance with the protocol ISO 11464. In brief, three repeated soil profiles at each site were hand-dug, and five depths in each of recognizable horizons (0–100 cm) were divided according to the primary aspects except for the forest site where seven layers from 0 to 70 cm depth were collected. The soil samples were air-dried at room temperature and sieved <2 mm to remove plant residues and coarser particles, then thorough mixed and pulverized by an agate mortar to pass through a 100–mesh (149 μm) Nylon screen for elemental analysis.

The soil samples were digested with a mixture of hydrochloric acid (HCl) –HNO_3–HF–perchloric acid ($HClO_4$) to measure the total concentrations of elements. After cooling, HNO_3 was added to the residue, and then the solutions were diluted to 25 mL with double-distilled deionized water before analysis. Analyses were performed by using Inductively Coupled Plasma-Atomic Emission Spectrometer (ICP-AES) and Atomic Absorption spectrometry (AAS). Quality control was assured by the analysis of duplicate samples, blanks and National Standard Materials (soil: GBW07403, GSS-3). The analysis results of the reference materials fluctuated within the allowable ranges of the certified values and the relative standard deviation of the duplicate analysis were less than the allowed upper-limits of the National Technical Specification for Soil Environmental Monitoring (HJ/T 166-2004).

3 Results and discussion

3.1 Dry deposition of TEs

3.1.1 Profile of dry-deposited TEs

Fig. 3 shows the annual mean $_{ddf}$TEs at the ten sites during the observation period. In general, the magnitude of $_{ddf}$TEs for each element at one station varied substantially, ranging from 0.03 mg m^{-2} yr^{-1} for Ag at the XL site to 10.3 g m^{-2} yr^{-1} for Al at the BD site. When the 25 TEs at each site were roughly identified using enrichment factors (EFs) relative to the average crustal composition with Al as a reference (Duce et al., 1975; Mason and Morre, 1982), only Pb, Zn, Cd, As, Se, Ag and Sb had EFs above 10, suggesting that the fluxes of these TEs were substantially affected by human activities. The primarily crustal elements with EFs lower than 10 (e.g., Al, Ca and Fe) had the highest flux among the 25 TEs. These TEs had fluxes similar to each other; the next highest fluxes were attributed to Na, Mg, K, Mn and Ba. Among dry-deposited particles, Zn was the most abundant anthropogenic metal, followed by Pb, Sb, Cu, Ni, Cr, As, Co, V, Se, Mo, Cd and Tl. Ag had the lowest measured flux among the heavy metals. In general, the average fluxes of the above crustal elements excepting Mn and Ba were 2−4 orders of magnitude higher than those of anthropogenic elements (e.g., Zn, As and Tl). The profile of TEs in dry-deposited particles agrees closely with those described in previous studies (Odabasi et al., 2002; Tasdemir and Kural, 2005). In addition, the dry deposition fluxes of most of the TEs in Northern China, as shown in Fig. 3, fell within the range of values reported within and outside China (Table 2), with the exception of some crustal elements (e.g., Na, Mg and Al). The relatively high dry deposition fluxes of crustal elements are not surprising because these elements are commonly found in the bare soil of the study area, which constitutes the major proportion of the particulate matter (Chen et al., 2014). Although accounting for only a small fraction of the particles, heavy metals are of great environmental importance due to their toxicity and anthropogenic origins (Almeida et al., 2006). In conclusion, the dry deposition of TEs originating from both regional natural and local anthropogenic sources is closely linked to the dry nature of the soil and the intensive human activities in Northern China.

3.1.2 Spatial variation in $_{ddf}$TEs

Generally, the values of $_{ddf}$TEs were significantly higher for urban and industrial sites (e.g., BD, TJ and TS) compared with suburban, agricultural and rural sites (e.g., CZ, YC and XL). For example, the three-year mean $_{ddf}$Pb was largest at BD (35.6 mg m^{-2} yr^{-1}), followed by TS, TG and TJ (31.4, 27.3, 23.1 mg m^{-2} yr^{-1}, respectively). The $_{ddf}$Pb was similar at YF, LC and BJ, with high values of 17.8, 13.6 and 13.2 mg m^{-2} yr^{-1}, respectively. At CZ, YC and XL, the $_{ddf}$Pb was relatively low (7.1, 7.1 and 5.7 mg m^{-2} yr^{-1}, respectively). This spatial pattern was closely linked with local emissions, implying that human activities have affected the dry deposition of TEs and altered their regional budget, particularly for heavy metals. The human impact is more pronounced at the industrial sites of BD and TS. As shown clearly in Fig. 3, the dry deposition of some elements was significantly elevated at BD (Al, Be, Pb, Se, Th, Tl, U, V, Cd, Co, As, Mo, Ba, Sb and Cu) or TS (Fe, Mn, Mg, V, K, Ca, Ag and Cr) compared with at other urban or industrial sites. This finding suggests the presence of substantial metal emissions near these two sites. At TS, for example, the highest depositions of Fe, Mn and Cr were observed, which can be attributed primarily to the iron and steel processing industry, particularly the relocation of the Capital Steel Company from Beijing to Tangshan City during the observation period. After this relocation, a substantial decline in airborne steel-related elements has been observed in Beijing (Chen et al., 2014).

The two pairs of urban-suburban sites located in the Beijing and Tianjin metropolitan areas allowed us to assess the spatial variation in dry deposition along the environmental gradient. As expected, the dry deposition fluxes of most elements in the megacity, TJ, were higher than those in its suburban counterpart, TG, excepting certain elements such as Mn, Pb, Sb, Cu, Co, Ni and Cr. The relatively high $_{\mathrm{ddf}}$TEs observed at TG reflect the industrial activities in the coastal regions near Tianjin Harbor. This pattern is supported by the fact that the pre-2001 Pb level in the coastal waters of Bohai Bay originated primarily from river discharge; after 2001, a declining trend has not been observed due to additional contributions from atmospheric deposition, although the annual runoff levels have declined (Meng et al., 2008). Another recent geochemical study also suggested the contribution of atmospheric inputs of harmful elements to the surface sediments of Bohai Bay (Duan et al., 2010). These findings further indicate the human impact on regional element cycling, particularly on the transport and deposition from inland to coastal areas.

Compared with other sites, certain elements were found at the highest or second highest levels at TJ (Zn, Na, As, Cr and Tl) and TG (Ni, Cr, Pb and Mn). Wet deposition of Zn at TJ and Ni at TG was also higher than at other sites (Fig. 3). Relatively high values of certain TEs observed in both wet and dry deposition may indicate special non-ferrous smelters near the site. However, the dry deposition fluxes of some TEs (Mo, As, Tl, Se, Be, Th and U) at TG was relatively low compared with other industrial sites and was comparable to rural sites, suggesting that industry related to these TEs was lacking at TG. Therefore, careful attention must be paid to source apportionment in the future.

The dry deposition fluxes of most elements at another megacity (BJ) were comparable to or lower than those of its suburban counterpart, YF, and also lower than those of other urban and industrial sites. The low values at BJ can be attributed to the restrictions on industrial sources in the fourth rings of Beijing City. In addition, the YF site lies 30 km NW of BJ, where there are some local sources. As a consequence, the $_{\mathrm{ddf}}$TEs of Al, K, Pb, Tl, Cd, V, As and Zn were higher at YF than at BJ and were comparable to other industrial sites, highlighting the influence of human activities on dry deposition in suburban areas.

Interestingly, the dry deposition fluxes of some heavy metals (Zn, Cd and Pb) at LC were higher than those at another agricultural site (YC) and comparable to other urban or industrial sites. These elevated heavy metals observed in dry-deposited particles at LC may be due to industrial plumes emitted from Shijiazhuang City (SJZ), the capital of Hebei Province. This conjecture is supported by the fact that the highest values of dry-deposited sulfate were observed at this site (Pan et al., 2013b). Although the $_{\mathrm{ddf}}$TEs at the rural XL site were the lowest in the target area, they were still comparable to or higher than the measurements given in Table 2. This finding indicates that the $_{\mathrm{ddf}}$TEs in the target region were high and that more attention must be paid to their harmful impacts on ecosystems and human health in Northern China.

3.1.3 Seasonal variations in $_{\mathrm{ddf}}$TEs

The seasonal mean $_{\mathrm{ddf}}$TEs during the three-year period are also shown in Fig. 3. The $_{\mathrm{ddf}}$TEs exhibited similar seasonal variations at most sites, with higher values observed in spring/winter than in summer/autumn. In the target areas, the meteorological conditions during cold seasons are often dry with low precipitation. In addition, strong northwest winds and the lack of vegetation may favor the resuspension of soil particles in the atmosphere, resulting in the increased dry deposition of crustal elements (Chen et al., 2014). With the exception of BD and TS, most sites in this study suffered from the regional transport of natural dust, especially during spring. This effect is more pronounced at the rural and agricultural sites XL, YC, CZ and YF, where natural sources dominated the fluxes.

To confirm the influences of regional dust, we checked the Sand-Dust Weather Almanac issued by the Chinese Meteorological Administration and found that there were 31 sand-dust weather events recorded in China between 2008 and 2010. Of the total, 16 events (9 events occurred in spring) reached the target regions during the period; all of which were blowing or floating dust and no sand-storms were recorded. We thus conclude that the long-range transport of natural dust from the northern/northwestern deserts and loess deposits resulted in the relatively high dry deposited elemental flux in spring than in other seasons in this study. In addition, sand-dust weather events decreased eastward due to the effects of distance and particle size. As a result, there were more days with blowing or floating dust at BJ than at east coastal site of TG, according to the recorded weather phenomena. Dry deposition of Al at these two sites (2.1 and 1.3 g m^{-2}) during spring also supported this phenomenon. Moreover, with the exception of Cu, Sb and Ba, the dry deposition elemental fluxes at the BJ site in spring are relatively high compared with the other seasons, coinciding with more days with blowing or floating dust at BJ than at other sites.

At industrial sites of BD and TS, however, the seasonal distribution of most TEs, except for crustal elements, were relatively high in winter compared with in spring. In addition to the low precipitation, the increased emission strength from coal burning in cold seasons is a major contributor. In Northern China coal is still the primary fuel widely used for industrial processes and daily life, and more coal is combusted for heating in winter. Thus, dry depositions in winter were expected to be enhanced in the region where a great deal of coal was combusted. This is supported by the elevated flux of various TEs at the urban and industrial sites of TJ, BD and TS, compared with that in other sites. The enhanced fluxes of heavy metals (e.g., Pb and Tl) in winter at

TG and LC are also related to coal consumption. In the urban areas of Beijing, however, the energy used for heating and industrial processes was mainly electricity and natural gas in addition to limited residential coal consumption (Zhao et al., 2013). At present, annual coal consumption in Beijing was about 21 million tons, which is significantly lower than that in Tianjin and Hebei (70 and 300 million tons). As a consequence, the dry deposition of coal combustion related TEs (e.g., Pb and Tl) in BJ was lower than that in TJ, BD and TS, but still higher than that in YC, CZ and XL, indicating the influences of residential coal consumption in the urban areas of Beijing. In the past ten years with the gradual replacement of coal by natural gas and electricity in urban Beijing, the sulfate and elemental carbon in the winter decreased gradually from 25 and 8.7 μg m^{-3} to 14 and 6.3 μg m^{-3}, respectively (Zhao et al., 2013). Further decrease of elemental deposition in Beijing can be expected, if the reduction of coal consumption continues.

In contrast, the minimum fluxes observed in the summer/autumn are attributable to an increase in precipitation. Wet soil conditions and vegetation cover also decrease the amount of re-suspended particles in the atmosphere. The above analysis demonstrates that the $_{ddf}$TEs varied from one season to another due to changes in meteorological conditions and human-induced emissions in addition to the seasonal variation in natural sources.

3.2 Wet deposition of TEs

3.2.1 Profile of TEs in precipitation

Fig. 3 shows the annual mean $_{wdf}$TEs at the ten sites during the observation period. The magnitude of $_{wdf}$TEs for each element at one station varied significantly, from 0.01 mg m^{-2} yr^{-1} for Th at the XL site to 3.1 g m^{-2} yr^{-1} for Ca at the YF site. Of the primarily crustal elements, Ca exhibited the highest flux, followed by Na, Mg and K. Zn was found to be the most abundant anthropogenic metal in wet deposition, followed by Pb, Sb, Cu, As, Co, Se, Ni, V, Cr, Mo, Cd and Tl. In general, the average fluxes of the above crustal elements were several times higher than those of Mn, Ba, Fe and Al, and 2−4 orders of magnitude greater than those of the anthropogenic elements (e.g., As, Cd and Tl). The profile of TEs in wet deposition determined in this study agrees well with those described in previous reports (Halstead et al., 2000; Hu and Balasubramanian, 2003). In addition, the wet deposition of Cd, Cr, Co, Ni and V in Northern China, as shown in Fig. 3, was comparable to that observed in other sites listed in Table 3. In contrast, the wet deposition of Fe, Al, Mn and Zn was higher in Northern China than in other regions of the world. The $_{\text{wdf}}$Pb was also higher in this study than previously reported, with the exception of the North Sea and Singapore (Table 3). The relatively high $_{\text{wdf}}$TEs may be attributable to anthropogenic influences in addition to natural emissions, considering that the EFs of the majority of TEs in wet deposition at each site were above 10, with the exceptions of Be, K, Na, Mg, Al, Fe, Ni, Cr, V, Th and U. However, the calculation of EFs on the basis of Al was most probably overestimated because the crustal elements were not dissolved completely in the acidified precipitation samples, as discussed in Sect. 2.3.1.

Since the $_{\text{wdf}}$Pb was higher in this study than that in most of the previously reports, one may be interested in the major sources of Pb in the region. Besides natural sources from regional and local soil, possible anthropogenic sources of Pb include coal combustion, vehicle exhaust, cement factories and smelters (Cheng and Hu, 2010). But the relative contribution of the above sources was of spatial and temporal variable. After the phase-out of leaded gasoline in China since 2000, the major emission sources of airborne Pb in eastern and central China were estimated to be coal consumption and non-ferrous metal smelting, instead of vehicle exhaust (Li et al., 2012). However, detailed Pb isotopic signatures of PM_{10} from selected sites in North China indicated its source was mainly anthropogenic, and mostly attributable to coal combustion and vehicle emissions with additional industrial sources (Luo et al., 2014). A case study in Beijing found that airborne Pb predominantly from anthropogenic sources was reduced by approximately 50% during the 2008 Olympic Games due to the mitigation measures implemented by the Chinese Government (Schleicher et al., 2012). Moreover, the temporal variations of Pb concentration correlated to the restrictiveness of relative measures, especially during different traffic restrictions, further demonstrating the significance of traffic sources (Chen et al., 2014). But the vehicular emissions from urban areas (e.g., Beijing) were not likely an important regional source of Pb and thus had insignificant impacts in rural areas (e.g., Xianghe) (Li et al., 2010). We conclude that Pb in wet deposition on the regional scale was mainly emitted from industrial processes and coal burning. These emissions could be widely dispersed throughout the atmosphere and transported to the downwind regions (Zhao et al., 2013), resulting in the high wet depositions at the background site of XL (discussed in Sect. 3.2.3).

3.2.2 Seasonal variations in $_{\mathrm{wdf}}$TEs

The seasonal variations in $_{\mathrm{wdf}}$TEs showed similar trends at each site (Fig. 3), with a maximum in summer coinciding with the rainy season in Northern China. The minimum values obtained in the winter months were attributable to the low level of precipitation. In general, summer contributed the most to the annual wet deposition flux, followed by spring, autumn and winter. A significant linear correlation between the wet deposition flux and precipitation was observed at each site for heavy metals such as Cu, Pb, Zn, Cd, As and Se. Therefore, precipitation is important in explaining the seasonal pattern of the above TEs collected at a given site. However, this is not the case for most crustal elements (e.g., Al, Mn, Fe, Na and Ba), which exhibit less of a correlation between the $_{\mathrm{wdf}}$TEs and precipitation (Fig. S5). This finding suggests that the wet deposition of these metals is more closely related to their concentration in the precipitation than to the precipitation amount.

Although the precipitation in winter was comparable at each site, the spatial variation of $_{\mathrm{wdf}}$TEs in the cold season was evident. For example, the wet deposition of Al, Fe, Be, U, Mn, V and Cr showed substantially higher values at TJ, BD, TG, TS and CZ compared with the other sites, indicating different emission strengths among the sites.

3.2.3 Spatial variation in $_{wdf}$TEs

In general, the spatial distribution of $_{wdf}$TEs exhibited less variation. For example, the three-year mean $_{wdf}$Pb was highest at TG (10.1 mg m^{-2} yr^{-1}), followed by TS, BD and YC (10.0, 9.9 and 9.2 mg m^{-2} yr^{-1}, respectively). The $_{ddf}$Pb was similar at CZ, XL, LC, TJ and BJ, with high results of 8.8, 8.4, 8.2, 8.0 and 6.4 mg m^{-2} yr^{-1}, respectively. The lowest value occurred at YF (3.9 mg m^{-2} yr^{-1}). This pattern is different from the dry-deposited TEs, for which higher values were found at industrial and urban sites than at suburban, agricultural and rural areas. The wet deposition of certain elements (e.g., Al, Mg, Mn, Se, Th, U, V, Ca, Cd, Ag, Ni, Zn and Cr), however, was somewhat higher at the industrial sites compared with the other sites, indicating that these TEs were affected by local emissions. In Germany, heavy metals were also found to be higher in precipitation in urban–industrial areas than at rural measurement sites (Grömping et al., 1997). Surprisingly, unlike the dry-deposited TEs found in low values at XL, the wet deposition of certain TEs (e.g., Ag, Co, K, Be, Pb, Sb, Th and U) at XL was comparable to or higher than that at other sites, including industrial sites. Since there were no local emission sources near XL, the higher $_{wdf}$TEs most likely resulted from the long-range transport from upwind areas of Northern China (Pan et al., 2013a). The long-range transport effects on wet deposition flux of TEs were recorded elsewhere. For example, wet deposition fluxes of TEs measured along the Japan Sea coast were strongly affected by the long-range transport of air pollutants from the Asian continent during winter and spring (Sakata et al., 2006). A recent study also found that long-range transport of pollutants from south Asia had a significant impact on the trace elements in atmospheric wet deposition in the high altitude remote areas in the southern slope of the Himalayas (Tripathee et al., 2014).

Since the emissions of industrial pollutants and fossil fuel combustion from upwind sources in Tianjin and Hebei are prominent, trace elements in precipitation observed at XL could be from regional emission sources. Imprints of regional transport were indicated by the fact that the metallic episodes experienced at the XL site closely associated with the air mass from SE that passed TS and TJ, or from SW that passed BD and SJZ. It is reasonable because trace elements associated with fine particles can remain in the atmosphere for days or weeks and thus be subject to long-range transboundary transport. They are therefore widely dispersed throughout the atmosphere before they finally deposit through washout by precipitation (below-cloud scavenging) in remote regions (Duce et al., 1975). In addition, aerosols acting as host for the trace elements can enter cloud water mainly through rainout (in-cloud scavenging) and be transported to downwind regions far away from sources (Levkov et al., 1991). Although both rainout and washout pathways contributed to the wet deposition of trace elements, their relative importance during the long-range transport has not been well characterized. Therefore, there is a need for further research to better understand the long-range transport of pollutants from potential source regions with the atmospheric circulation in Northern China.

3.2.4 Factors influencing the regional distribution of $_{wdf}$TEs

To investigate the factors controlling the regional distributions of $_{wdf}$TEs, the scavenging ratio (S_r) was introduced under the simplified assumption that the concentration of a component in precipitation (C_p) is related to the concentration of the respective compound in the air (C_a) (Sakata et al., 2006). Thus, S_r can be calculated on a mass basis as follows:

$$S_r = C_p/C_a. \tag{1}$$

When the precipitation volume is expressed as P, the $_{wdf}$TEs depend on S_r, C_a and P:

$$_{wdf}TEs = S_rC_aP. \tag{2}$$

Therefore, if S_r and C_a are constant in the region, $_{wdf}$TEs increase in proportion to P. However, for sites with higher values of C_a, $_{wdf}$TEs were greater than expected from P based on the above premise (i.e., S_rC_a = constant). Thus, by using the relationship between $_{wdf}$TEs and P, we can evaluate the degree to which $_{wdf}$TEs are governed by anthropogenic emissions at each site.

The statistical analysis of data from the three-year period revealed a positive relationship between the annual wet deposition fluxes of 12 trace elements (As, Cd, Co, Cu, Fe, Mn, Pb, Sb, Se, Th, Tl and V) and the corresponding precipitation volume ($0.11 < r^2 < 0.38$; Fig. S5). For most of these TEs that exist entirely as fine particles that can act as condensation nuclei, this finding may indicate that wet deposition represents a large contribution of their long-range transport during in-cloud processes. However, only approximately 20% of the variance in the wet deposition fluxes for these TEs is explained by the volume of precipitation. The aforementioned percentage is significantly lower than that estimated in Japan, e.g., 68% and 80% of the variance in $_{wdf}$Sb and $_{wdf}$V is explained using the precipitation volume (Sakata et al., 2006), suggesting marked differences in the S_r and C_a of TEs across Northern China. For example, the $_{wdf}$Pb values at the BD, LC and TS sites in certain years was much higher than expected based on the precipitation amount, indicating a large contribution from anthropogenic emissions. However, the relatively low $_{wdf}$Pb values at the YC, CZ and YF sites compared with those expected from the precipitation amount may be due to the lower number of anthropogenic sources in suburban areas.

In contrast, the relationship between the annual wet deposition fluxes and the precipitation amount for the rest of the 13 TEs (Zn, U, Ni, Na, Mo, Mg, K, Cr, Ca, Ba, Be, Al and Ag) is not significant (Fig. S5). The results demonstrate that the annual values of these TEs were most likely dominated by the scavenging ratio and atmospheric concentrations across Northern China. Clearly, there is marked difference in the atmospheric concentrations of these TEs throughout the study region (Pan et al., 2013a; Zhao et al., 2013), although the available data are not sufficient. Considering that these TEs exist entirely in coarse particulate form, their wet deposition depends on the below-cloud scavenging of local emissions rather than regional contributions. For TEs in fine particles, however, wet deposition is mainly governed by regional transport (most of which might be from in-cloud scavenging) rather than local emissions.

3.3 Total deposition of TEs

3.3.1 Wet vs. dry deposition of TEs

A comparison of the $_{wdf}$TEs and $_{ddf}$TEs at each site provided in Fig. 3 shows that the dry deposition fluxes of most TEs were significantly higher than their wet deposition values. For example, dry-deposited Cu, Al, Fe, Mn and V dominated the total deposition flux at each site. In contrast, the wet deposition fluxes of K, Ni and As exceeded their dry deposition fluxes at only a single site (XL or YC). For Pb, Zn, Cd, Se, Ag and Tl, however, the relative importance between their wet and dry deposition fluxes varied site by site. The wet deposition of these TEs tended to dominate the total deposition flux at BJ, CZ, YC and XL.

The relative significance of wet vs. dry deposition may change not only based on the efficiencies of the two mechanisms but also with the local availability of precipitation (Muezzinoglu and Cizmecioglu, 2006). In Germany, more than 90% of the total metal amount was reported to exist as wet deposition, and wet deposition is thought to be the predominant mechanism for the removal of ecotoxicologically relevant metals in high latitudes (Grömping et al., 1997). In contrast, dry deposition as a cleansing mechanism is the most important on an annual basis in semi-arid regions with low precipitation (Grantz et al., 2003). This pattern has been verified in a Mediterranean climate area (Muezzinoglu and Cizmecioglu, 2006) and partially verified in this study.

The relative difference between $_{wdf}$TEs and $_{ddf}$TEs is likely due to the difference in the size distributions of TEs in atmospheric particles. Sakata et al. (2008) reported that the wet deposition fluxes of Pb and Se in Japan exceeded their dry deposition fluxes, whereas the reverse was true for Cr, Cu, Mn, Mo, Ni and V. The authors also found that the difference between the wet and dry deposition fluxes of As, Cd and Sb varied by site. Finally, they concluded that the dry deposition of TEs associated with larger particles is expected to be greater than their wet deposition fluxes because coarse particles have much shorter atmospheric lifetimes due to their higher deposition velocities (Sakata and Marumoto, 2004). In contrast, wet deposition may dominate the total flux for TEs exist as fine particles, which act as condensation nuclei for the formation of precipitation.

To confirm the above hypothesis, we performed elemental analyses on size-resolved particles collected at five selected sites (BD, BJ, TJ, TS and XL). The results showed that Al, Fe, Th and U were concentrated in coarse particles, whereas Cu, Pb, Zn, Cd, As, Se, Ag and Tl mainly existed as fine particles (Fig. 4). In addition, the size distributions of Be, Na, K, Ca, Ba, Mg, Co, V, Mo, Ni, Sb, Cr and Mn were bimodal at all sites, with two peaks at 0.43–0.65 μm and 4.7–5.8 μm and a valley at 1.1–2.1 μm (Fig. 4). The above premise proposed by Sakata et al. (2008) is partially supported by our measurements indicating that the dry deposition fluxes of TEs associated with larger particles (e.g., Al, Mn and Fe) are larger than their wet deposition fluxes. Similarly, the TEs accumulated in fine particles (e.g., As, Pb and Cd) have much larger wet deposition than dry deposition fluxes.

Interestingly, however, some metals have a similar size distribution but different deposition mechanisms (e.g., Cu and Pb). This circumstance may be due to the different solubilities of these TEs because the solubility determines the release of metals from particles and their subsequent incorporation into rainwater (Desboeufs et al., 2005). Although the solubility of Cu (43–93%) is comparable to that of Pb (40–93%) in most studies, only 8.4% of Cu was soluble in rainwater sampled at Istanbul (Cizmecioglu and Muezzinoglu, 2008). Thus, the low solubility of Cu may be the cause for the low wet deposition fluxes. However, this premise was not verified in the study (e.g., at the BJ site). We did not measure the distribution of Cu and Pb between liquid and solid phases in precipitation, but we can examine the solubility of metals based on the experiments a and c described in Sect. 2.3.1 for the 10 precipitation samples at the BJ site. The results showed that the solubility of Cu (26%) was higher than that of Pb (7%), suggesting that the deposition mechanisms of the two metals were not influenced by the solubility. After carefully checking the size distribution of particles at the BJ site we found that Cu had another peak around 4.7-5.8 μm in addition to that at 0.43-0.65 μm (Fig. 4). In contrast, there is only one peak at 0.43-0.65 μm for Pb. Thus, the different deposition mechanisms of Cu and Pb can be well explained by the size distribution.

3.3.2 Wet plus dry deposition of TEs

The annual total (wet plus dry) deposition fluxes of the TEs ($_{tdf}$TEs) at ten sites in Northern China are indicated in Table 4. The 25 measured TEs in Northern China had total deposition fluxes ranging from 101 to 404 kg ha^{-1} yr^{-1}, with a ten-site average of 236±98 kg ha^{-1} yr^{-1} during the three-year period. The lowest and highest $_{tdf}$TEs were observed for Ag at the CZ site (0.05 mg m^{-2} yr^{-1}) and Ca at the TS site (138 kg ka^{-1} yr^{-1}), respectively.

The spatial variation in $_{tdf}$TEs was similar to that of dry deposition; the values at LC and YF were higher than those at XL, YC and CZ and lower than those at BJ, TJ, BD, TG and TS. In most cases, the $_{tdf}$TEs for industrial and urban sites were highest, followed by agricultural, suburban and rural sites (e.g., Pb; Fig. 1). Although it is difficult to compare the $_{tdf}$TEs type by type due to the limited available measurement data for the study region, the relatively high $_{tdf}$TEs observed for land use types other than rural areas stem from increased TEs emissions. Most importantly, the $_{tdf}$TEs measured at XL, which can be used as a reference to characterize the background level in Northern China, were still relatively high compared with those of remote regions around the world (Table 5). Thus, the extremely high $_{tdf}$TEs observed in the target areas compared with those reported both within and outside China can be easily understood. Notably, the current deposition fluxes at the XL site (Table 3), which is located in a forest area surrounded by few villages, exceeds the critical load of Pb (7.0 mg m^{-2} yr^{-1}) calculated for Dutch forest soils (de Vries et al., 1998). However, this is not the case for the other heavy metals (Cu, Zn and Cd). Although nationwide emissions of TEs from power plants have gradually declined in recent years, Northern China still ranks among the regions that will have the highest emissions in the coming decades (Tian et al., 2014). This result raises important concerns regarding the potential effects of substantial metal deposition on different ecosystems. Therefore, it is important to further reduce the emissions to mitigate the environmental risks posed by TEs in Northern China.

3.3.3 Atmospheric deposition of TEs into ecosystems

To quantify the contribution of atmospheric deposition to the elemental level in receiving ecosystems, it is necessary to know the metal content of a specific surface area for comparison with the atmospheric deposition in the same area. The mass content (M_c, mg m^{-2}) of TEs in the vertical soil profile is determined according to the following equation:

$$M_c = 10D_lB_dC_s \tag{3}$$

where 10 is the conversion coefficient and D_1, B_d and C_s are depth (cm), bulk density (g cm^{-3}) and the metal concentration (mg kg^{-1}) in each vertical layer, respectively.

In this study, we selected two agricultural sites (LC and YC) and a forest site approximately 100 km to the west of Beijing (BJF), where the elemental content of a typical soil profile (0−100cm) was measured in 2005. Only 11 TEs (Mo, Mn, Zn, Cu, Fe, Se, Cd, Pb, Cr, Ni and As) were selected because the other TEs were not available in the soil profile. The distribution of M_c for each metal vs. soil depth was first examined (Fig. 5). At the LC site, the M_c of Mn, Fe and As increased with depth, whereas that of Mo, Zn, Cr and Ni was enriched at 20−40 cm. In addition, Cu, Se and Pb were slightly accumulated in the top soil of 0−10 cm. No systematic pattern was found for Cd, which was rather stable within the profile. At the YC site, Zn, Se and Pb contents were found highest in the surface soil and decreased generally with depth. Mo, Mn, Cu, Fe, Cd, Cr, Ni and As were enriched in the plow horizon from 40−60 cm, which is deeper than that for Mo, Zn, Cr and Ni found at LC. Note that the M_c of each metal (except for Cr) in the forest soils of Beijing increases with depth (Fig. 5).

For TEs whose M_c increase with depth, the trend appears to be largely related to the parent materials of the soils at each site. Alternatively, the enrichment of TEs in the top soil may suggest important sources (e.g., atmospheric deposition) other than the mineralization of indigenous minerals. Presuming that the top soil (0−10 cm) and deep soil (60−100 cm) had the same initial elemental content when riverine alluvial soil was formed at the location, the significant enrichment of TEs in the upper soil layer indicates an anthropogenic origin such as atmospheric deposition, plant litter decomposition, fertilizer application or sewage irrigation.

The increase in elemental content (mg m^{-2}) in the topsoil (0−10 cm) relative to the deep soil (60−100 cm), which indicates the total anthropogenic input, is calculated and listed in Table 6. The ratio of atmospheric deposition to the total anthropogenic input (R_{at}) varied among sites and TEs. Negative values may indicate negligible anthropogenic input compared with the mineralization input. The R_{at} values for Mo, Zn, Cu, Se, Cd and Pb at YC were 0.02, 0.20, 0.01, 0.03, 1.03 and 0.05, respectively, indicating that atmospheric deposition contributed 20% of anthropogenic Zn and almost all of the Cd in the topsoil. The explanation for the R_{at} values lower than 0.05 are not clear at present and require further study.

At another agricultural site (YC), the R_{at} values of Mn, Zn, Cu, Se, Cd, Pb, Cr and As were 0.01, 0.03, 0.78, 0.11, 0.18, 0.05, 0.01 and 0.10, respectively. Thus, atmospheric deposition accounted for 10−78% of the anthropogenic Cu, Se, Cd and As input. Although the R_{at} of some TEs was lower than 0.05, the contribution of atmospheric input cannot be overlooked when considering a longer accumulation period. A national inventory estimated that the inputs of TEs (As, Cr, Ni and Pb) to agricultural soils via atmospheric deposition were 43–85% (Luo et al., 2009). Thus, long-term parallel measurements of atmospheric deposition and soil profile physico-chemical properties are required to detect the accumulated impacts. In addition, the chemical speciation and bioavailability of atmospheric deposited TEs should be considered given that the mobility of TEs determines their transformation and accumulation from soil and water to plants and humans.

As fertilization practices are not applicable in natural ecosystems, forest, for example, may be an ideal upland ecosystems in which to track atmospheric deposition (Hovmand et al., 2008). However, the increasing elemental M_c with depth in the forest soils of Beijing makes it difficult to quantify the anthropogenic input using the method described above. Nevertheless, impacts of atmospheric deposition on the urban park and agricultural soils were identified in Beijing (Chen et al., 2005; Lu et al., 2012). Evidence can also be found at the rural forest site of XL, where elevated elemental concentrations were observed in fine particles transported via southern winds from industrial and urban areas in Northern China (Pan et al., 2013a).

4 Conclusions

To our knowledge, this study provides the first long-term direct measurements of atmospheric wet and dry deposition fluxes of crustal and anthropogenic metals on a regional scale across China. The dataset provides a basis for the validation of regional emission inventories and biogeochemical or atmospheric chemistry models. It also facilitates the effective targeting of policies to protect ecosystems (e.g., water and soils) from long-term heavy metal accumulation. Three major findings and conclusions can be drawn:

1. Significantly higher $_{ddf}$TEs were observed at industrial and urban areas than at suburban, agricultural and rural sites, corresponding to the urban-rural land use gradient. The minimum $_{ddf}$TEs that occurred in summer/autumn were attributable to an increase in precipitation, whereas the maximum in winter/spring were due to the additional emissions from coal burning and regional transport of natural dust. Elevated $_{ddf}$TEs, most of which originated from coarse particles, are closely linked with the regional dry nature of the soil and the intensive local human activities in Northern China.
2. Due to the precipitation pattern in Northern China, summer contributed the most to annual wet deposition flux, followed by spring, autumn and winter. Although the precipitation in winter was comparable at each site, the spatial variation in the wet deposition fluxes of several TEs in cold season was evident due to the local emissions from house heating. Compared with $_{ddf}$TEs, however, the annual $_{wdf}$TEs had less spatial variation and were influenced by the regional patterns of precipitation and emissions. The wet deposition of TEs that exist as fine particles was mainly governed by regional transport rather than local emissions. However,

for coarse particulate TEs, wet deposition was attributed mainly to below-cloud scavenging (most of which might be from local emissions).

3. The relative importance between wet and dry deposition flux varied among sites and TEs. Nevertheless, dry deposition flux was significantly higher than the wet deposition flux for most TEs, signifying the dominance of self-cleansing mechanisms in the atmosphere. In addition to the local availability of precipitation, size distribution of TEs in particles is also an important factor determining the relative importance of wet vs. dry deposition. Compared with other measurements around the world, the atmospheric deposition flux in Northern China was very high, indicating that the mitigation of metal emissions is greatly needed in the future.

The case study demonstrates that a comparison of atmospheric deposition and vertical soil profile is an appropriate tool with which to characterize the atmospheric input of toxic metals to ecosystems and to differentiate their contributions from other anthropogenic sources. The atmospheric deposition of Cu, Pb, Zn, Cd, As and Se is of the same magnitude as the increase of these TEs in the topsoil; this type of atmospheric deposition may dominate the anthropogenic input to agricultural systems in the future. Our study further highlights the need to focus on the chemical speciation and bioavailability of atmospherically deposited materials and demonstrates the importance of establishing long-term observation studies on the accumulation of heavy metals in food chains as a result of substantial atmospheric deposition.

Acknowledgments

This work was supported by the “Strategic Priority Research Program” of the Chinese Academy of Sciences (No.: XDB05020000 & XDA05100100), the National Basic Research Program of China (No.: 2012CB417101 & 2012CB417106) and the National Natural Science Foundation of China (No.: 41405144, 41230642 & 41321064). The authors are indebted to the site operators who collected the samples for this project and the Chinese Ecosystem Research Network (CERN) providing the metal data in soil profile observed at the Yucheng, Luancheng and Beijing forest stations. Special thanks go to X. Zhu, L. Wang, S. Tian and G. Zhang for their valuable assistance in preparation of the original manuscript.

References

Almeida, S. M., Pio, C. A., Freitas, M. C., Reis, M. A., and Trancoso, M. A.: Approaching $PM_{2.5}$ and $PM_{2.5-10}$ source apportionment by mass balance analysis, principal component analysis and particle size distribution, Sci. Total. Environ., 368, 663-674, doi:10.1016/j.scitotenv.2006.03.031, 2006.

Chaemfa, C., Barber, J. L., Kim, K.-S., Harner, T., and Jones, K. C.: Further studies on the uptake of persistent organic pollutants (POPs) by polyurethane foam disk passive air samplers, Atmos. Environ., 43, 3843-3849, doi:10.1016/j.atmosenv.2009.05.020, 2009a.

Chaemfa, C., Wild, E., Davison, B., Barber, J. L., and Jones, K. C.: A study of aerosol entrapment and the influence of wind speed, chamber design and foam density on polyurethane foam passive air samplers used for persistent organic pollutants, J. Environ. Monitor., 11, 1135-1139, doi:10.1039/B823016A, 2009b.

Chen, T. B., Zheng, Y. M., Lei, M., Huang, Z. C., Wu, H. T., Chen, H., Fan, K. K., Yu, K., Wu, X., and Tian, Q. Z.: Assessment of heavy metal pollution in surface soils of urban parks in Beijing, China, Chemosphere, 60, 542-551, doi:10.1016/j.chemosphere.2004.12.072, 2005.

Chen, Y., Schleicher, N., Chen, Y., Chai, F., and Norra, S.: The influence of governmental mitigation measures on contamination characteristics of $PM_{2.5}$ in Beijing, Sci. Total. Environ., 490, 647-658, doi:10.1016/j.scitotenv.2014.05.049, 2014.

Cheng, H., and Hu, Y.: Lead (Pb) isotopic fingerprinting and its applications in lead pollution studies in China: A review, Environ. Pollut., 158, 1134-1146, doi:10.1016/j.envpol.2009.12.028, 2010.

Chester, R., Nimmo, M., and Preston, M. R.: The trace metal chemistry of atmospheric dry deposition samples collected at Cap Ferrat: a coastal site in the Western Mediterranean, Mar. Chem., 68, 15-30, doi:10.1016/S0304-4203(99)00062-6, 1999.

Church, T. M., Veron, A., Patterson, C. C., Settle, D., Erel, Y., Maring, H. R., and Flegal, A. R.: Trace elements in the North Atlantic troposphere: shipboard results of precipitation and aerosols, Global. Biogeochem. Cy, 4, 431-443, doi:10.1029/GB004i004p00431, 1984.

Cizmecioglu, S. C., and Muezzinoglu, A.: Solubility of deposited airborne heavy metals, Atmos. Res., 89, 396-404, doi:10.1016/j.atmosres.2008.03.012, 2008.

Cong, Z., Kang, S., Zhang, Y., and Li, X.: Atmospheric wet deposition of trace elements to central Tibetan Plateau, Appl. Geochem., 25, 1415-1421, doi:10.1016/j.apgeochem.2010.06.011, 2010.

Dasch, J. M.: Direct measurement of dry deposition to a polyethylene bucket and various surrogate surfaces, Environ. Sci. Technol., 19, 721-725, doi:10.1021/es00138a011, 1985.

de Vries, W., Bakker, D. J., Groenenberg, J. E., Reinds, G. J., Bril, J., and van Jaarsveld, J. A.: Calculation and mapping of critical loads for heavy metals and persistent organic pollutants for Dutch forest soils, J. Hazard. Mater., 61, 99-106, doi:10.1016/S0304-3894(98)00113-7, 1998.

Desboeufs, K. V., Sofikitis, A., Losno, R., Colin, J. L., and Ausset, P.: Dissolution and solubility of trace metals from natural and anthropogenic aerosol particulate matter, Chemosphere, 58, 195-203, doi:10.1016/j.chemosphere.2004.02.025, 2005.

Duan, L., Song, J., Xu, Y., Li, X., and Zhang, Y.: The distribution, enrichment and source of potential harmful elements in surface sediments of Bohai Bay, North China, J. Hazard. Mater., 183, 155-164, doi:10.1016/j.jhazmat.2010.07.005, 2010.

Duce, R. A., Hoffman, G. L., and Zoller, W. H.: Atmospheric trace metals at remote northern and southern hemisphere sites: Pollution or natural?, Science, 187, 59-61, doi:10.1016/0029-554X(81)90639-X, 1975.

Duce, R. A., Liss, P. S., Merrill, J. T., Atlas, E. L., and Buat-Menard, P.: The atmospheric input of trace species to the world ocean, Global. Biogeochem. Cy, 5, 193-259, doi:10.1029/91GB01778, 1991.

Fang, G. C.: A study of mass size distributions and particle deposition velocities in ambient air, Ph.D.Thesis of Illinois Institute of Technology, Illinois Institute of Technology, Chicago, 220 pp., 1992.

Golomb, D., Ryan, D., Eby, N., Underhill, J., and Zemba, S.: Atmospheric deposition of toxics onto Massachusetts Bay-I. Metals, Atmos. Environ., 31, 1349-1359, doi:10.1016/S1352-2310(96)00276-2, 1997.

Grömping, A. H. J., Ostapczuk, P., and Emons, H.: Wet deposition in Germany: Long-term trends and the contribution of heavy metals, Chemosphere, 34, 2227-2236, doi:10.1016/S0045-6535(97)00080-5, 1997.

Grantz, D. A., Garner, J. H. B., and Johnson, D. W.: Ecological effects of particulate matter, Environ. Int., 29, 213-239, doi:10.1016/S0160-4120(02)00181-2, 2003.

Guieu, C., Chester, R., Nimmo, M., Martin, J., Guerzoni, S., Nicolas, E., Mateu, J., and Keyse, S.: Atmospheric input of dissolved and particulate metals to the northwestern Mediterranean, Deep Sea Research Part II: Topical Studies in Oceanography, 44, 655-674, doi:10.1016/S0967-0645(97)88508-6, 1997.

Halstead, M. J. R., Cunninghame, R. G., and Hunter, K. A.: Wet deposition of trace metals to a remote site in Fiordland, New Zealand, Atmos. Environ., 34, 665-676, doi:10.1016/S1352-2310(99)00185-5, 2000.

Harner, T., Shoeib, M., Diamond, M., Stern, G., and Rosenberg, B.: Using Passive Air Samplers To Assess Urban-Rural Trends for Persistent Organic Pollutants. 1. Polychlorinated Biphenyls and Organochlorine Pesticides, Environ. Sci. Technol., 38, 4474-4483, doi:10.1021/es040302r, 2004.

Heal, M. R., Hibbs, L. R., Agius, R. M., and Beverland, I. J.: Total and water-soluble trace metal content of urban background PM_{10}, $PM_{2.5}$ and black smoke in Edinburgh, UK, Atmos. Environ., 39, 1417-1430, doi:10.1016/j.atmosenv.2004.11.026, 2005.

Herut, B., Nimmo, M., Medway, A., Chester, R., and Krom, M. D.: Dry atmospheric inputs of trace metals at the Mediterranean coast of Israel (SE Mediterranean): sources and fluxes, Atmos. Environ., 35, 803-813, doi:10.1016/S1352-2310(00)00216-8, 2001.

Hovmand, M. F., Kemp, K., Kystol, J., Johnsen, I., Riis-Nielsen, T., and Pacyna, J. M.: Atmospheric heavy metal deposition accumulated in rural forest soils of southern Scandinavia, Environ. Pollut., 155, 537-541, doi:10.1016/j.envpol.2008.01.047, 2008.

Hovmand, M. F., Nielsen, S. P., and Johnsen, I.: Root uptake of lead by Norway spruce grown on ^{210}Pb spiked soils, Environ. Pollut., 157, 404-409, doi:10.1016/j.envpol.2008.09.038, 2009.

Hsu, S. C., Wong, G. T. F., Gong, G.-C., Shiah, F. K., Huang, Y. T., Kao, S. J., Tsai, F., Candice Lung, S. C., Lin, F. J., Lin, I. I., Hung, C. C., and Tseng, C. M.: Sources, solubility, and dry deposition of aerosol trace elements over the East China Sea, Mar. Chem., 120, 116-127, doi:10.1016/j.marchem.2008.10.003, 2010.

Hu, G. P., and Balasubramanian, R.: Wet deposition of trace metals in Singapore, Water Air. Soil Poll., 144, 285-300, doi:10.1023/A:1022921418383, 2003.

Huang, X. F., Li, X., He, L. Y., Feng, N., Hu, M., Niu, Y. W., and Zeng, L. W.: 5-Year study of rainwater chemistry in a coastal mega-city in South China, Atmos. Res., 97, 185-193, doi:10.1016/j.atmosres.2010.03.027, 2010.

Injuk, J., Grieken, R. V., and Leeuw, G. D.: Deposition of atmospheric trace elements into the north sea: Coastal, ship, platform measurements and model predictions, Atmos. Environ., 32, 3011-3025, doi:10.1016/S1352-2310(97)00497-4, 1998.

Kaya, G., and Tuncel, G.: Trace element and major ion composition of wet and dry depositon in Ankara, Turkey, Atmos. Environ., 31, 3985-3998, doi:10.1016/s1352-2310(97)00221-5, 1997.

Kim, G., Scudlark, J. R., and Church, T. M.: Atmospheric wet deposition of trace elements to Chesapeake and Delaware Bays, Atmos. Environ., 34, 3437-3444, doi:10.1016/S1352-2310(99)00371-4, 2000.

Kim, J.-E., Han, Y.-J., Kim, P.-R., and Holsen, T. M.: Factors influencing atmospheric wet deposition of trace elements in rural Korea, Atmos. Res., 116, 185-194, doi:10.1016/j.atmosres.2012.04.013, 2012.

Kyllönen, K., Karlsson, V., and Ruoho-Airola, T.: Trace element deposition and trends during a ten year period in Finland, Sci. Total. Environ., 407, 2260-2269, doi:10.1016/j.scitotenv.2008.11.045, 2009.

Levkov, L., Eppel, D. P., and Graβl, H.: Modelling the atmospheric transport of trace metals including the role of precipitating clouds, Atmos. Environ., 25, 779-789, doi:10.1016/0960-1686(91)90076-J, 1991.

Li, C., Wen, T., Li, Z., Dickerson, R. R., Yang, Y., Zhao, Y., Wang, Y., and Tsay, S.-C.: Concentrations and origins of atmospheric lead and other trace species at a rural site in northern China, J. Geophys. Res., 115, D00K23, doi:10.1029/2009JD013639, 2010.

Li, Q., Cheng, H., Zhou, T., Lin, C., and Guo, S.: The estimated atmospheric lead emissions in China, 1990–2009, Atmos. Environ., 60, 1-8, doi:10.1016/j.atmosenv.2012.06.025, 2012.

Lindberg, S. E., and Harriss, R. C.: The role of atmospheric deposition in an eastern U.S. deciduous forest, Water, Air, and Soil Pollution, 16, 13-31, doi:10.1007/BF01047039, 1981.

Liu, C. L., Zhang, J., and Yu, Z. G.: Study on the characteristics of the aerosol and atmospheric flux of the heavy metals over the Yellow Sea, Mar. Environ. Sci., 17, 1-6 (in Chinese), 1998.

Liu, C. L., Ren, H. B., Chen, H. T., and Xia, N.: Heavy metals in precipitation from the Yellow Sea and the East China Sea Regions, Mar. Sci., 27, 64-68 (in Chinese), 2003.

Lu, A., Wang, J., Qin, X., Wang, K., Han, P., and Zhang, S.: Multivariate and geostatistical analyses of the spatial distribution and origin of heavy metals in the agricultural soils in Shunyi, Beijing, China, Sci. Total. Environ., 425, 66-74, doi:10.1016/j.scitotenv.2012.03.003, 2012.

Luo, L., Ma, Y. B., Zhang, S. Z., Wei, D. P., and Zhu, Y. G.: An inventory of trace element inputs to agricultural soils in China, J. Environ. Manage., 90, 2524-2530, doi:10.1016/j.jenvman.2009.01.011, 2009.

Luo, X. S., Ip, C. C. M., Li, W., Tao, S., and Li, X. D.: Spatial–temporal variations, sources, and transport of airborne inhalable metals (PM_{10}) in urban and rural areas of northern China, Atmos. Chem. Phys. Discuss., 14, 13133-13165, doi:10.5194/acpd-14-13133-2014, 2014.

Mason, B., and Morre, C. B.: Principles of geochemistry, Wiley, New York, 344 pp., 1982.

McTainsh, G. H., Nickling, W. G., and Lynch, A. W.: Dust deposition and particle size in Mali, West Africa, Catena., 29, 307-322, doi: 10.1016/S0341-8162(96)00075-6, 1997.

Meng, W., Qin, Y., Zheng, B., and Zhang, L.: Heavy metal pollution in Tianjin Bohai Bay, China, J. Environ. Sci., 20, 814-819, doi:10.1016/S1001-0742(08)62131-2, 2008.

Momani, K. A., Jiries, A. G., and Jaradat, Q. M.: Atmospheric deposition of Pb, Zn, Cu, and Cd in Amman, Jordan, Turk. J. Chem., 24, 231-238, 2000.

Morselli, L., Brusori, B., Passarini, F., Bernardi, E., Francaviglia, R., Gataleta, L., Marchionni, M., Aromolo, R., Benedetti, A., and Olivieri, P.: Heavy metals monitoring at a Mediterranean natural ecosystem of Central Italy. Trends in different environmental matrixes, Environ. Int., 30, 173-181, doi:10.1016/S0160-4120(03)00170-3, 2004.

Motelay-Massei, A., Ollivon, D., Tiphagne, K., and Garban, B.: Atmospheric bulk deposition of trace metals to the Seine river Basin, France: concentrations, sources and evolution from 1988 to 2001 in Paris, Water Air. Soil Poll., 164, 119-135, doi:10.1007/s11270-005-1659-x, 2005.

Muezzinoglu, A., and Cizmecioglu, S. C.: Deposition of heavy metals in a Mediterranean climate area, Atmos. Res., 81, 1-16, doi:10.1016/j.atmosres.2005.10.004, 2006.

Nguyen, V. D., Merks, A. G. A., and Valenta, P.: Atmospheric deposition of acid, heavy metals, dissolved organic carbon and nutrients in the Dutch delta area in 1980-1986, Sci. Total. Environ., 99, 77-91, doi:10.1016/0048-9697(90)90213-E, 1990.

Noll, K. E., Fang, K. Y. P., and Watkins, L. A.: Characterization of the deposition of particles from the atmosphere to a flat plate, Atmos. Environ., 22, 1461-1468, doi:10.1016/0004-6981(88)90170-9, 1988.

Odabasi, M., Muezzinoglu, A., and Bozlaker, A.: Ambient concentrations and dry deposition fluxes of trace elements in Izmir, Turkey, Atmos. Environ., 36, 5841-5851, doi:10.1016/S1352-2310(02)00644-1, 2002.

Okubo, A., Takeda, S., and Obata, H.: Atmospheric deposition of trace metals to the western North Pacific Ocean observed at coastal station in Japan, Atmos. Res., 129–130, 20-32, doi:10.1016/j.atmosres.2013.03.014, 2013.

Pan, Y. P., Wang, Y. S., Xin, J. Y., Tang, G. Q., Song, T., Wang, Y. H., Li, X. R., and Wu, F. K.: Study on dissolved organic carbon in precipitation in Northern China, Atmos. Environ., 44, 2350-2357, doi:10.1016/j.atmosenv.2010.03.033, 2010a.

Pan, Y. P., Wang, Y. S., Yang, Y. J., Wu, D., Xin, J. Y., and Fan, W. Y.: Determination of trace metals in atmospheric dry deposition with a heavy matrix of PUF by inductively coupled plasma mass spectroscopy after microwave digestion, Environ. Sci., 31, 553-559 (in Chinese), 2010b.

Pan, Y. P., Wang, Y. S., Tang, G. Q., and Wu, D.: Wet and dry deposition of atmospheric nitrogen at ten sites in Northern China, Atmos. Chem. Phys., 12, 6515-6535, doi:10.5194/acp-12-6515-2012, 2012.

Pan, Y. P., Wang, Y. S., Sun, Y., Tian, S. L., and Cheng, M. T.: Size-resolved aerosol trace elements at a rural mountainous site in Northern China: importance of regional transport, Sci. Total. Environ., 461, 761-771, doi:10.1016/j.scitotenv.2013.04.065, 2013a.

Pan, Y. P., Wang, Y. S., Tang, G. Q., and Wu, D.: Spatial distribution and temporal variations of atmospheric sulfur deposition in Northern China: insights into the potential acidification risks, Atmos. Chem. Phys., 13, 1675-1688, doi:10.5194/acp-13-1675-2013, 2013b.

Pike, S. M., and Moran, S. B.: Trace elements in aerosol and precipitation at New Castle, NH, USA, Atmos. Environ., 35, 3361-3366, doi:10.1016/S1352-2310(00)00525-2, 2001.

Sakata, M., and Marumoto, K.: Dry deposition fluxes and deposition velocities of trace metals in the Tokyo metropolitan area measured with a water surface sampler, Environ. Sci. Technol., 38, 2190-2197, doi:10.1021/es030467k, 2004.

Sakata, M., Marumoto, K., Narukawa, M., and Asakura, K.: Regional variations in wet and dry deposition fluxes of trace elements in Japan, Atmos. Environ., 40, 521-531, doi:10.1016/j.atmosenv.2005.09.066, 2006.

Sakata, M., Tani, Y., and Takagi, T.: Wet and dry deposition fluxes of trace elements in Tokyo Bay, Atmos. Environ., 42, 5913-5922, doi:10.1016/j.atmosenv.2008.03.027, 2008.

Sakata, M., and Asakura, K.: Factors contributing to seasonal variations in wet deposition fluxes of trace elements at sites along Japan Sea coast, Atmos. Environ., 43, 3867-3875, doi:10.1016/j.atmosenv.2009.05.001, 2009.

Sakata, M., and Asakura, K.: Atmospheric dry deposition of trace elements at a site on Asian-continent side of Japan, Atmos. Environ., 45, 1075-1083, doi:10.1016/j.atmosenv.2010.11.043, 2011.

Sandroni, V., and Migon, C.: Atmospheric deposition of metallic pollutants over the Ligurian Sea: labile and residual inputs, Chemosphere, 47, 753-764, doi:10.1016/S0045-6535(01)00337-X, 2002.

Schleicher, N., Norra, S., Chen, Y., Chai, F., and Wang, S.: Efficiency of mitigation measures to reduce particulate air pollution—A case study during the Olympic Summer Games 2008 in Beijing, China, Sci. Total. Environ., 427–428, 146-158, doi:10.1016/j.scitotenv.2012.04.004, 2012.

Shannigrahi, A. S., Fukushima, T., and Ozaki, N.: Comparison of different methods for measuring dry deposition fluxes of particulate matter and polycyclic aromatic hydrocarbons (PAHs) in the ambient air, Atmos. Environ., 39, 653-662, doi:10.1016/j.atmosenv.2004.10.025, 2005.

Shoeib, M., and Harner, T.: Characterization and Comparison of Three Passive Air Samplers for Persistent Organic Pollutants, Environ. Sci. Technol., 36, 4142-4151, doi:10.1021/es020635t, 2002.

Sweet, C. W., Weiss, A., and Vermette, S. J.: Atmospheric deposition of tace metals at three sites near the Great Lakes, Water Air. Soil Poll., 103, 423-439, doi:10.1023/A:1004905832617, 1998.

Takeda, K., Marumoto, K., Minamikawa, T., Sakugawa, H., and Fujiwara, K.: Three-year determination of trace metals and the lead isotope ratio in rain and snow depositions collected in Higashi-Hiroshima, Japan, Atmos. Environ., 34, 4525-4535, doi:10.1016/S1352-2310(00)00103-5, 2000.

Tasdemir, Y., and Kural, C.: Atmospheric dry deposition fluxes of trace elements measured in Bursa, Turkey, Environ. Pollut., 138, 462-472, doi:10.1016/j.envpol.2005.04.012, 2005.

Theodosi, C., Stavrakakis, S., Koulaki, F., Stavrakaki, I., Moncheva, S., Papathanasiou, E., Sanchez-Vidal, A., Koçak, M., and Mihalopoulos, N.: The significance of atmospheric inputs of major and trace metals to the Black Sea, J. Marine. Syst., 109–110, 94-102, doi:10.1016/j.jmarsys.2012.02.016, 2013.

Tian, H., Liu, K., Zhou, J., Lu, L., Hao, J., Qiu, P., Gao, J., Zhu, C., Wang, K., and Hua, S.: Atmospheric emission inventory of hazardous trace elements from China’s coal-fired power plants—temporal trends and spatial variation characteristics, Environ. Sci. Technol., 48, 3575-3582, doi:10.1021/es404730j, 2014.

Tripathee, L., Kang, S., Huang, J., Sharma, C. M., Sillanpää, M., Guo, J., and Paudyal, R.: Concentrations of trace elements in wet deposition over the Central Himalayas, Nepal, Atmos. Environ., 95, 231-238, doi:10.1016/j.atmosenv.2014.06.043, 2014.

Wang, Y., Li, P. H., Li, H. L., Liu, X. H., and Wang, W. X.: PAHs distribution in precipitation at Mount Taishan: China. Identification of sources and meteorological influences, Atmos.

Res., 95, 1-7, doi:10.1016/j.atmosres.2009.07.011, 2010.

Wang, Y., Yu, W., Pan, Y., and Wu, D.: Acid neutralization of precipitation in Northern China, J. Air Waste Manage., 62, 204-211, doi:10.1080/10473289.2011.640761, 2012.

Wang, Y., Peng, Y., Wang, D., and Zhang, C.: Wet deposition fluxes of total mercury and methylmercury in core urban areas, Chongqing, China, Atmos. Environ., 92, 87-96, doi:10.1016/j.atmosenv.2014.03.059, 2014.

Wesely, M., and Hicks, B.: A review of the current status of knowledge on dry deposition, Atmos. Environ., 34, 2261-2282, 2000.

Williams, M. R., Millward, G. E., Nimmo, M., and Fones, G.: Fluxes of Cu, Pb and Mn to the north-eastern Irish Sea: The importance of sedimental and atmospheric inputs, Mar. Pollut. Bull., 36, 366-375, doi:10.1016/S0025-326X(98)00199-4, 1998.

Wong, C. S. C., Li, X. D., Zhang, G., Qi, S. H., and Peng, X. Z.: Atmospheric deposition of heavy metals in the Pearl River Delta, China, Atmos. Environ., 37, 767-776, doi:10.1016/S1352-2310(02)00929-9, 2003.

Wu, C. X., Qi, S. H., Su, Q. K., Fang, M., and Wang, W.: Atmospheric deposition of heavy metals to Xinghua Bay, Fujian province, Environ. Chem., 25, 781-784 (in Chinese), 2006.

Yang, F., Tan, J., Shi, Z. B., Cai, Y., He, K., Ma, Y., Duan, F., Okuda, T., Tanaka, S., and Chen, G.: Five-year record of atmospheric precipitation chemistry in urban Beijing, China, Atmos. Chem. Phys., 12, 2025-2035, doi:10.5194/acp-12-2025-2012, 2012.

Yi, S. M., Lee, E. Y., and Holsen, T. M.: Dry deposition fluxes and size distributions of heavy metals in Seoul, Korea during Yellow-Sand events, Aerosol. Sci. Tech., 35, 569-576, doi:10.1080/02786820120775, 2001a.

Yi, S. M., Shahin, U., Sivadechathep, J., Sofuoglu, S. C., and Holsen, T. M.: Overall elemental dry deposition velocities measured around Lake Michigan, Atmos. Environ., 35, 1133-1140, doi:10.1016/S1352-2310(00)00242-9, 2001b.

Zhang, L., Fang, G. C., Liu, C. K., Huang, Y. L., Huang, J. H., and Huang, C. S.: Dry deposition fluxes and deposition velocities of seven trace metal species at five sites in central Taiwan – a summary of surrogate surface measurements and a comparison with model estimations, Atmos. Chem. Phys., 12, 3405-3417, doi:10.5194/acp-12-3405-2012, 2012.

Zhang, Q., Streets, D. G., Carmichael, G. R., He, K. B., Huo, H., Kannari, A., Klimont, Z., Park, I. S., Reddy, S., and Fu, J. S.: Asian emissions in 2006 for the NASA INTEX-B mission, Atmos. Chem. Phys., 9, 5131-5153, doi:10.5194/acp-9-5131-2009, 2009.

Zhang, Y. L., Lee, X. Q., and Cao, F.: Chemical characteristics and sources of organic acids in precipitation at a semi-urban site in Southwest China, Atmos. Environ., 45, 413-419, doi:10.1016/j.atmosenv.2010.09.067, 2011.

Zhao, P. S., Dong, F., He, D., Zhao, X. J., Zhang, X. L., Zhang, W. Z., Yao, Q., and Liu, H. Y.: Characteristics of concentrations and chemical compositions for $PM_{2.5}$ in the region of Beijing, Tianjin, and Hebei, China, Atmos. Chem. Phys., 13, 4631-4644, doi:10.5194/acpd-13-863-2013, 2013.

Zheng, M., Guo, Z., Fang, M., Rahn, K. A., and Kester, D. R.: Dry and wet deposition of elements in Hong Kong, Mar. Chem., 97, 124-139, doi:10.1016/j.marchem.2005.05.007, 2005.

Tables

Table 1. Descriptions of the ten sampling sites in the wet and dry deposition observation network of Northern China.

Site	Coordinates	Classification	Location	Population density (persons km^{-2}) [a]	Surrounding environment [c]	Underlying surface [a]	Measurements height (m)
BJ	39.96°N, 116.36°E	Urban	North to the Beijing downtown	5479	Densely occupied residences and traffic roads	Roof	8
TJ	39.08°N, 117.21°E	Urban	South to the Tianjin downtown	24606	Densely occupied residences, industry and traffic roads	Lawn	1.5
BD	38.85°N, 115.50°E	Industrial	Centre of the Baoding city	2871	Densely occupied residences, traffic roads and industry	Roof	10.5
TG	39.04°N, 117.72°E	Industrial	30 km east to the Tianjin city (Tanggu district)	865	Light industry and traffic roads	Lawn	1.5
TS	39.60°N, 118.20°E	Industrial	South to the Tangshan city	2648	Densely occupied residences, traffic roads and industry	Roof	13.5
YF	40.15°N, 116.10°E	Suburban	40 km northwest to the Beijing city (Yangfang town)	470	Occupied residences and traffic roads	Grass	1.5
CZ	38.30°N, 116.87°E	Suburban	2 km southeast to the Cangzhou city	2314	Small villages and high ways	Roof	5.5

LC	37.89°N, 114.69°E	Agricultural	4 km southeast to the Shijiazhuang city (Luancheng county)	958	Small villages and cropland	Lawn	1.5
YC	36.85°N, 116.55°E	Agricultural	6 km southwest to the Yucheng city	521	Small villages and cropland	Lawn	1.5
XL	40.38°N, 117.57°E	Rural	Xinglong, on the Mt. Yan with an elevation of 960 m a.s.l. (Hebei Province)	98	Forest and few villages	Grass	1.5

[a] The population density was estimated by dividing population by area of the town/district/county in which the monitoring site is located. Population data were retrieved from the fifth census of China in 2000 and can be accessed online (http://www.stats.gov.cn).

Table 2. Atmospheric dry deposition fluxes of metals within and outside China (mg m^{-2} yr^{-1}, but kg ha^{-1} yr^{-1} for Na, Ca, Mg, Fe, Mn and Al)

Site	Period	Na	Ca	Mg	Al	Mn	Fe	Cu	Pb	Zn	Cd	Co	Ni	Cr	V	Reference
Xinghua Bay, China	2004-2005	6.69	/	/	7.83	/	6.83	2.71	3.83	14.39	0.08	0.28	7.82	11.63	/	(Wu et al., 2006)
Yellow sea, China	1995-1996	12.42	6.32	2.89	4.49	0.08	2.55	0.23	1.92	2.91	0.04	0.2	0.63	1.11	1	(Liu et al., 1998)
East Sea China	2005-2007	/	/	/	0.15	0.02	0.14	4.38	0.91	6.94	0.07	/	0.09	0.08	0.55	(Hsu et al., 2010)
Taiwan China	2009-2010	/	/	/	/	0.08	1.52	20.8	20.03	18.03	/	/	/	9.20	/	(Zhang et al., 2012)
Hong Kong ,China	1998-1999	6.67	/	1.15	0.83	0.07	0.78	5.25	28.98	27.95	/	/	/	/	0.19	(Zheng et al., 2005)
Matsuura, Japan	2004-2006	/	/	/	1.32	0.09	/	3.01	1.55	/	0.06	/	3.72	4.28	0.54	(Sakata and Asakura, 2011)
Seoul, S. Korea	Spring,1998	/	23.0	/	19.7	/	/	/	73.0	73.0	/	/	40.2	/	/	(Yi et al., 2001a)
Maagan Michale, Israel	1994-1997	/	/	/	4.97	0.11	4.32	0.23	1.54	1.98	0.07	/	/	1.27	/	(Herut et al., 2001)
Chicago, U.S.	1990s	/	25.51	9.12	/	0.4	/	69.4	46.4	266.5	4.4	/	/	19.3	/	(Fang, 1992)
Chicago, U.S.	1993-1995	/	/	8.29	3.80	0.21	/	23.0	13.87	43.80	/	/	/	2.08	1.21	(Yi et al., 2001b)
Sleeping Bear Dunes, U.S.	1993-1995	/	/	0.21	0.27	0.01	/	29.0	12.78	24.82	/	/	/	0.58	0.06	(Yi et al., 2001b)

South Heaven, U.S.	1993-1995	/	/	1.90	1.24	0.08	/	11.3	8.40	18.62	/	/	/	0.27	0.44	(Yi et al., 2001b)
Tor Paterno, Italy	1999	/	/	/	/	/	/	11.03	11.41	43.64	0.36	/	12.23	17.04	/	(Morselli et al., 2004)
Cap Ferat, France	1988-1989	/	/	/	1.20	0.02	0.88	1.19	1.85	3.20	/	0.02	0.33	0.38	/	(Chester et al., 1999)
Amman, Jordan	1995	/	/	/	/	/	/	5.55	4.20	29.69	0.15	/	/	/	/	(Momani et al., 2000)
Izmir, Turkey	2000-2001	/	157.32	11.32	/	0.49	44.13	45.3	80.3	697.2	8.8	/	47.1	5.8	/	(Odabasi et al., 2002)
Bursa, Turkey	2002-2003	/	88.44	12.88	/	0.62	29.23	71.17	55.84	366.46	1.10	2.92	46.36	22.26	/	(Tasdemir and Kural, 2005)

Table 3. Atmospheric wet deposition fluxes of metals within and outside China (mg m^{-2} yr^{-1}, but kg ha^{-1} yr^{-1} for Fe, Mn and Al)

Site	Period	Fe	Mn	Al	Cu	Pb	Zn	Cd	Cr	Co	Ni	V	Reference
Nam Co, central Tibetan Plateau, China	2007-2008	0.05	0.003	0.055	0.23	0.06	0.27	0.002	/	0.007	0.09	0.03	(Cong et al., 2010)
Hong Kong, China	1998-1999	0.78	0.04	0.62	4.67	86.94	33.15	/	/	/	/	2.65	(Zheng et al., 2005)
Yellow Sea, China	2000-2002	/	/	/	1.99	0.37	0.12	37.4	/	/	/	/	(Liu et al., 2003)
Kathmandu, Nepal	2011-2012	2.47	0.08	2.10	1.95	1.42	24.44	0.10	1.60	1.00	0.71	/	(Tripathee et al., 2014)
Dhunche, Nepal	2011-2012	1.00	0.04	0.98	0.02	0.02	0.18	0.00	0.00	0.01	0.02	/	(Tripathee et al., 2014)
Chuncheon, Korea	2006-2009	/	0.03	0.10	1.21	1.06	6.93	0.05	/	/	0.37	0.10	(Kim et al., 2012)
Nakanoto, Japan	2003-2005	/	0.07	/	1.8	10	27	0.31	0.40	/	1.40	0.78	(Sakata and Asakura, 2009)
Higashi-Hiroshima, Japan	1995–1997	/	0.02	<0.01	0.89	1.78	6.84	0.09	/	/	0.42	0.33	(Takeda et al., 2000)
Singapore	2000	0.62	0.07	0.48	14.56	8.84	18.72	0.78	4.16	1.56	10.14	9.10	(Hu and Balasubramanian, 2003)
Fiordland, New Zealand	1993–1995	3.70	0.001	/	0.02	0.04	0.07	0.00	/	/	/	/	(Halstead et al., 2000)
New Castle, U.S.	1996–1997	0.14	/	0.17	0.67	0.78	8.33	0.12	0.08	0.12	0.42	0.72	(Pike and Moran, 2001)
Chesapeake and Delaware Bay, U.S.	1995–1996	0.14	0.01	0.20	0.97	0.35	3.60	0.04	0.04	/	0.82	/	(Kim et al., 2000)
Massachusetts, U.S.	1992–1993	0.36	0.01	0.29	0.70	0.86	2.70	0.21	1.50	0.01	3.00	/	(Golomb et al., 1997)

Bermuda, U.S.	1982–1983	0.016	0.001	/	0.07	0.31	0.66	0.02	/	/	0.08	0.07	(Church et al., 1984)
Ankara, Turkey	1993–1994	0.007	/	0.003	0.45	0.87	2.84	1.32	0.16	/	0.20	0.21	(Kaya and Tuncel, 1997)
North Sea	1992–1994	/	/	/	10.50	11.00	31.00	/	1.40	/	/	/	(Injuk et al., 1998)
Dutch Delta, The Netherlands.	1990	/	/	/	0.23	4.23	12.67	0.07	/	/	0.88	/	(Nguyen et al., 1990)

Table 4. Atmospheric total deposition flux of metals in Northern China (mg m^{-2} yr^{-1})

Type	Urban		Industrial			Suburban		Agricultural		Rural	Regional	
Site	BJ	TJ	BD	TG	TS	YF	CZ	LC	YC	XL	Mean	SD
Ag	0.10	0.17	0.38	0.09	0.32	0.10	0.05	0.09	0.06	0.06	0.14	0.11
Be	0.21	0.38	0.64	0.22	0.31	0.23	0.13	0.12	0.10	0.07	0.24	0.17
Tl	0.22	0.34	0.47	0.20	0.36	0.26	0.18	0.17	0.15	0.13	0.25	0.11
U	0.28	0.48	1.27	0.30	0.46	0.31	0.19	0.19	0.17	0.11	0.38	0.34
Cd	0.46	0.56	0.98	0.50	0.61	0.49	0.43	0.64	0.39	0.29	0.54	0.19
Mo	0.69	0.94	1.82	0.68	0.80	0.56	0.50	0.46	0.63	0.26	0.73	0.42
Th	1.07	1.60	3.28	1.03	1.57	1.23	0.68	0.69	0.50	0.38	1.20	0.84
Se	1.47	1.96	4.07	1.85	2.47	1.64	1.53	1.53	1.40	1.14	1.90	0.84
Co	3.47	3.54	4.88	4.10	3.55	3.64	3.06	2.88	3.07	2.38	3.45	0.69
As	3.73	5.51	8.69	3.13	4.44	5.25	2.75	3.04	3.56	2.39	4.25	1.87
V	4.51	6.50	11.18	5.82	11.59	5.54	2.67	2.60	1.56	1.54	5.35	3.63
Cr	6.47	9.77	8.09	12.21	15.33	6.12	3.81	4.19	3.38	3.46	7.28	4.07
Ni	6.63	7.39	6.66	17.45	8.54	7.30	4.83	5.00	11.19	3.69	7.87	3.97
Cu	19.8	19.4	28.5	22.3	19.1	12.1	8.4	8.4	7.9	5.3	15.1	7.7

Pb	19.6	31.1	45.8	37.3	41.4	21.7	16.4	21.8	16.2	14.1	26.5	11.5
Sb	28.1	25.6	35.7	30.3	29.2	29.1	27.2	25.9	26.3	21.6	27.9	3.7
Mn	83.0	109.7	90.0	139.1	160.8	88.8	51.3	49.7	43.0	35.1	85.1	42.1
Ba	178.3	128.7	155.0	84.9	145.8	96.4	44.9	50.8	34.1	32.5	95.1	54.2
Zn	86.5	245.8	112.1	106.4	119.9	66.0	95.7	135.0	57.0	40.7	106.5	57.1
K	1841.1	2027.1	2341.1	1598.8	2495.3	2205.3	1173.3	1098.2	1100.0	1716.2	1759.6	516.4
Mg	2168.2	2999.2	2729.8	2778.6	3684.2	2258.8	1198.0	977.2	837.1	801.4	2043.3	1029.0
Na	2126.5	3021.5	1761.7	2383.4	2281.2	3145.1	2867.9	1314.9	1162.3	966.0	2103.1	784.6
Fe	3358.7	4604.3	4793.6	4386.8	10440.0	3644.1	2045.1	2453.0	2388.8	1456.8	3957.1	2547.7
Al	5076.8	6678.2	10337.2	4727.5	7179.3	5982.1	3269.0	3028.8	2297.3	1889.2	5046.5	2602.1
Ca	8807.5	11722.1	10493.5	10317.0	13777.1	8236.0	5511.8	5852.8	5516.0	3106.2	8334.0	3322.1
Sum	238.2	316.5	329.8	266.6	404.2	258.2	163.3	150.4	135.1	101.0	236.3	97.8

Sum denotes a total deposition flux of 25 TEs in Northern China, with the unit of kg ha^{-1} yr^{-1}

Table 5. Atmospheric total deposition fluxes of metals within and outside China (mg m^{-2} yr^{-1})

Site	Period	Cd	Cu	Ni	Pb	Zn	As	Mn	V	Reference
Pearl River Delta, China	2001–2002	/	18.6	/	12.7	104	/	/	2.1	(Wong et al., 2003)
Hong Kong ,China	1998-1999	/	9.92	/	115.92	61.1	/	10.29	2.84	(Zheng et al., 2005)
Kushiro, Japan	2008	0.02	0.56	0.72	0.98	4.02	/	4.74	/	(Okubo et al., 2013)
Tokyo Bay, Japan	2004-2005	0.39	16	6.8	9.9		2.9	87	6.9	(Sakata et al., 2008)
Virolahti, Finland	2007	0.04	1.00	0.14	1.1	3.8	0.09	2.3	0.36	(Kyllönen et al., 2009)
Paris, France	2001–2002	0.24	6	0.62	4.2	30	/	/	/	(Motelay-Massei et al., 2005)
Massachusetts Bay, US	1992–1993	0.27	2.5	1.5	1.8	7.8	0.02	3.4		(Golomb et al., 1997)
Chesapeake Bay, US	1992–1993	0.05	0.26	0.26	0.56	1.34	/	/	/	(Motelay-Massei et al., 2005)

Lake Superior, US	1993–1994	0.46	3.1	0.8	1.5	8.8	0.17	4.2	0.34	(Sweet et al., 1998)
Lake Michigan, US	1993–1994	0.45	1.9	0.61	1.6	6	0.14	2.8	0.14	(Sweet et al., 1998)
Lake Erie, US	1993–1994	0.49	4.2	0.74	1.8	17	/	/	/	(Sweet et al., 1998)
Fiorland, New Zealand	1993–1995	0.004	0.023	0.035	0.025	/	/	/	/	(Halstead et al., 2000)
Varna, Bulgaria, Black Sea	2008-2009	0.02	17.8	0.41	0.73	15.18	/	2.01	1.1	(Theodosi et al., 2013)
North Sea	1993–1994	/	1.24	/	3.52	6.5	0. 25	2.6	1.1	(Injuk et al., 1998)
Irish Sea	1993–1994	/	2.6	/	1.62	/	/	5.07	/	(Williams et al., 1998)
Mediterranean Coast	1988–1993	0.31	2.6	0.57	3.8	/	/	/	/	(Guieu et al., 1997)
Ligurian Sea	1997–1998	0.06	1.28	1.1	1.2	41.2	/	/	/	(Sandroni and Migon, 2002)

Table 6. Average enrichment (increment) of elemental content in top soil (0−10 cm) relative to deep soil (60−100 cm) vs. atmospheric total deposition flux of metals at agricultural sites on an annual basis (mg m^{-2})

Site	Item	Mo	Mn	Zn	Cu	Fe	Se	Cd	Pb	Cr	Ni	As
LC	Increment	22.3	-4684.6	662.1	749.4	-231178.5	43.6	0.6	420.8	-838.8	-349.7	-217.7
	Deposition	0.5	49.7	135.0	8.4	2453.0	1.5	0.6	21.8	4.2	5.0	3.0
	Ratio	**0.02**	**-0.01**	**0.20**	**0.01**	**-0.01**	**0.03**	**1.03**	**0.05**	**0.00**	**-0.01**	**-0.01**
YC	Increment	-12.8	3536.9	1709.3	10.1	-86889.7	13.0	2.1	347.4	232.5	-190.4	35.5
	Deposition	0.6	43.0	57.0	7.9	2388.8	1.4	0.4	16.2	3.4	11.2	3.6
	Ratio	**-0.05**	**0.01**	**0.03**	**0.78**	**-0.03**	**0.11**	**0.18**	**0.05**	**0.01**	**-0.06**	**0.10**

Data shown in bold was the ratio of total deposition to increment of metals in soil.

Figures

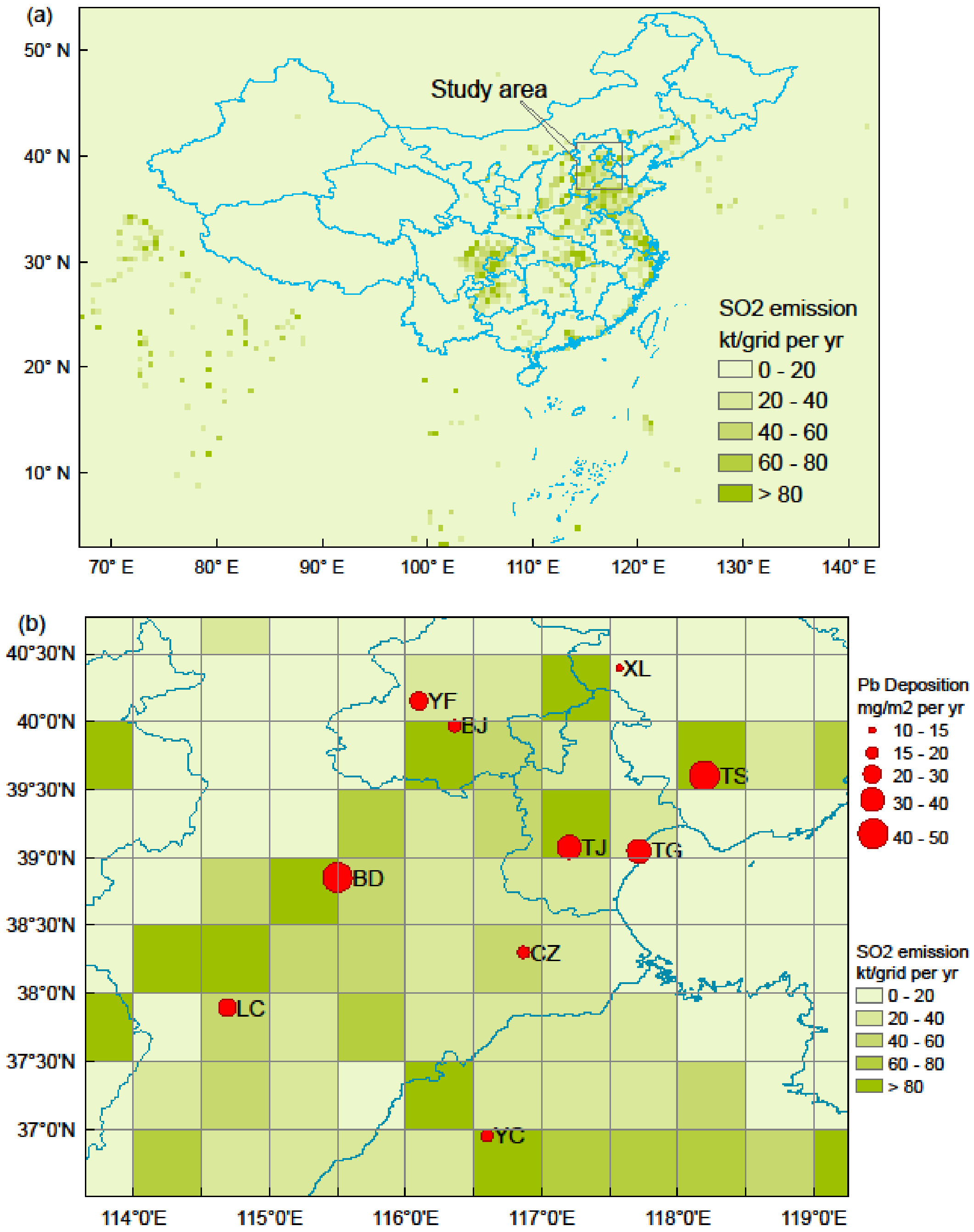

Fig. 1. Locations of the study area (a) and sampling sites (b) in Northern China with lead deposition and SO_2 emission distributions. The total lead deposition data are means of three-year observations from December 2007 to November 2010. The emission data for SO_2 are from 2006 (Zhang et al., 2009) and have a resolution of 0.5°×0.5°. In Northern China, the annual SO_2 emission unit of kt grid^{-1} is

approximately 400 mg m^{-2}.

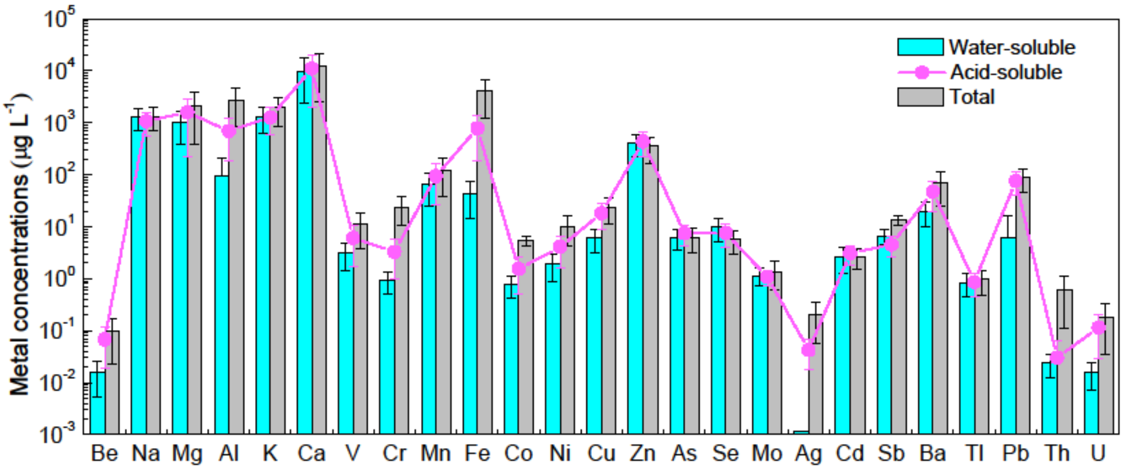

Fig. 2. The elemental abundance and fractions of precipitation collected in Beijing.

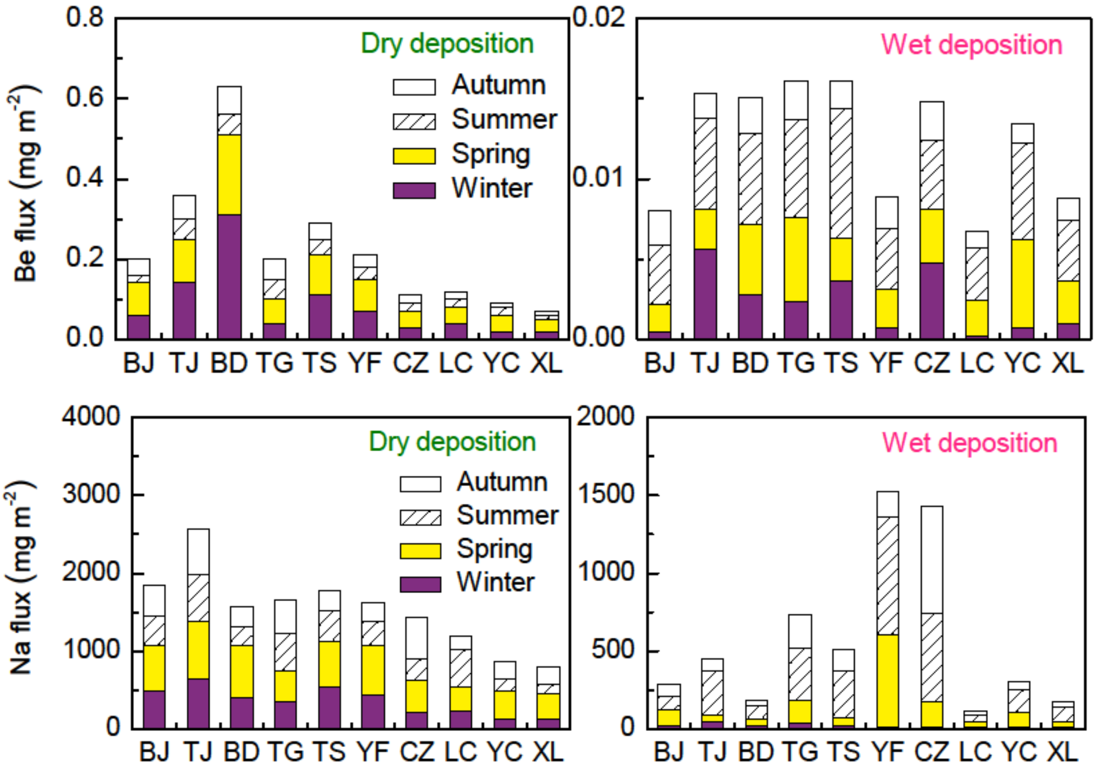

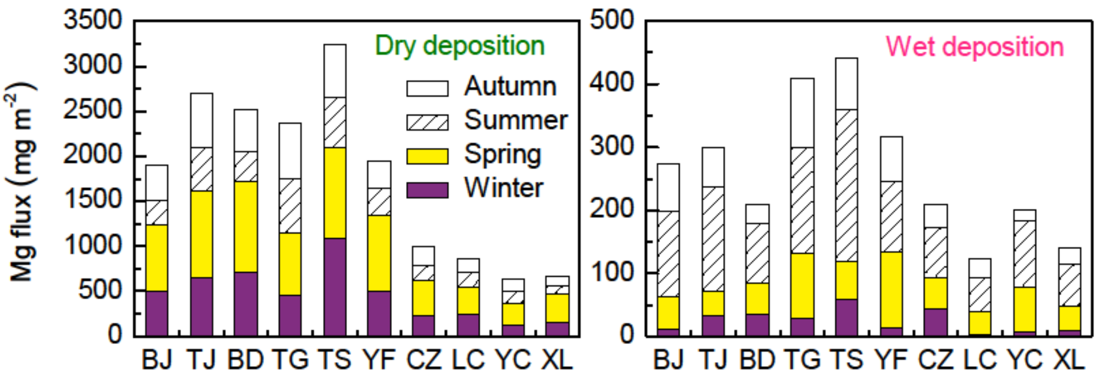
Mg flux (mg m^{-2})
3500
3000
2500
2000
1500
1000
500
0
Dry deposition
Autumn
Summer
Spring
Winter
BJ TJ BD TG TS YF CZ LC YC XL
500
400
300
200
100
0
Wet deposition
BJ TJ BD TG TS YF CZ LC YC XL

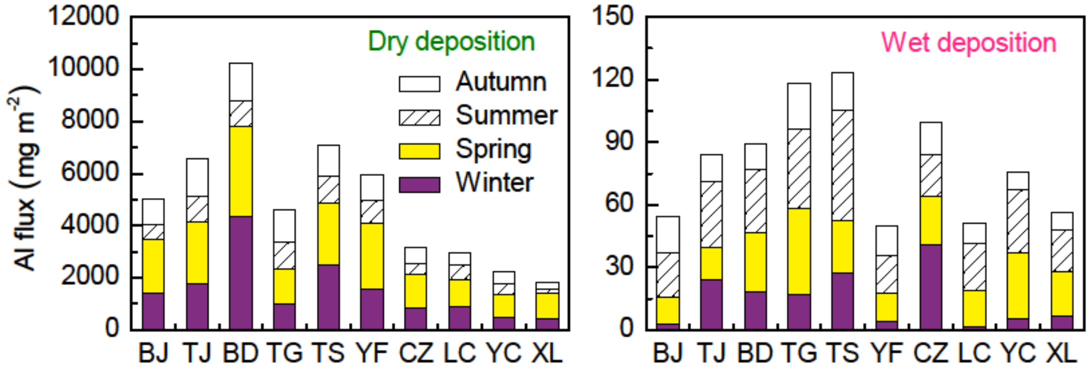
Al flux (mg m^{-2})
12000
10000
8000
6000
4000
2000
0
Dry deposition
Autumn
Summer
Spring
Winter
BJ TJ BD TG TS YF CZ LC YC XL
150
120
90
60
30
0
Wet deposition
BJ TJ BD TG TS YF CZ LC YC XL

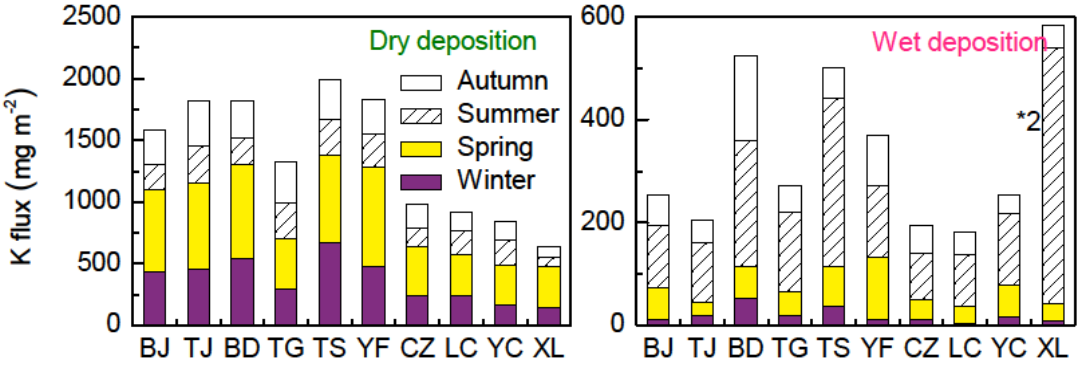
K flux (mg m^{-2})
2500
2000
1500
1000
500
0
Dry deposition
Autumn
Summer
Spring
Winter
BJ TJ BD TG TS YF CZ LC YC XL
600
400
200
0
Wet deposition
*2
BJ TJ BD TG TS YF CZ LC YC XL

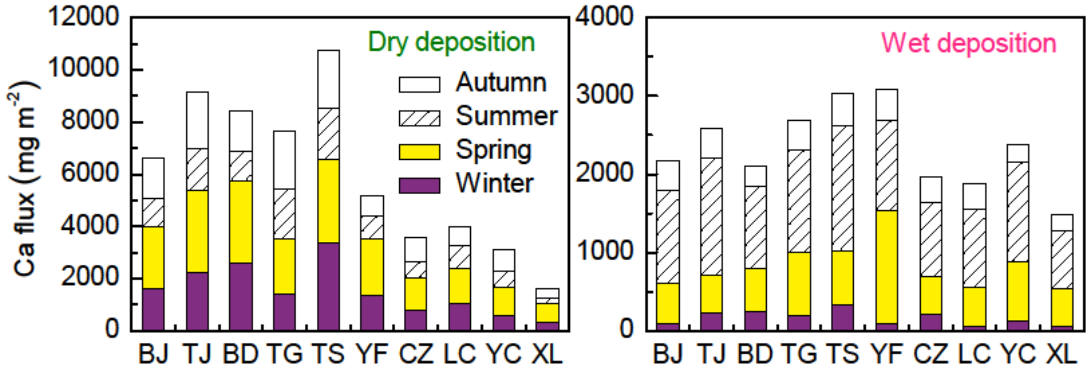
Ca flux (mg m^{-2})
12000
10000
8000
6000
4000
2000
0
Dry deposition
Autumn
Summer
Spring
Winter
BJ TJ BD TG TS YF CZ LC YC XL
4000
3000
2000
1000
0
Wet deposition
BJ TJ BD TG TS YF CZ LC YC XL

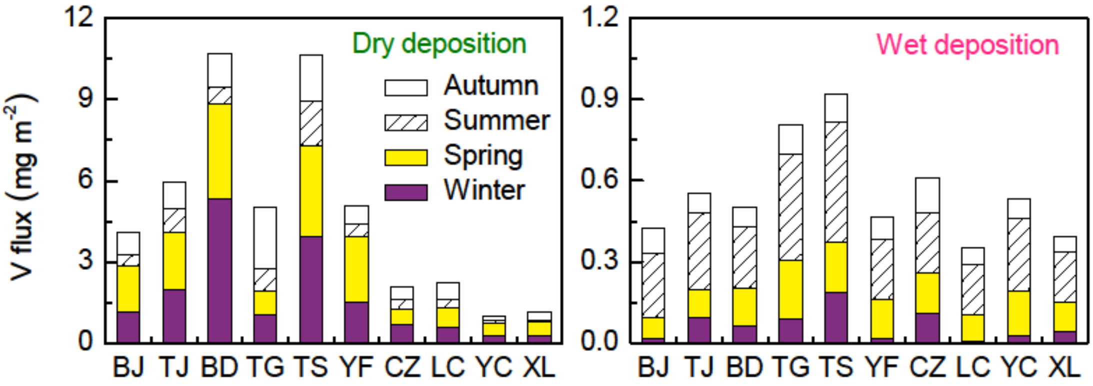
V flux (mg m^{-2})
Dry deposition
Autumn
Summer
Spring
Winter
Wet deposition
0
3
6
9
12
0.0
0.3
0.6
0.9
1.2
BJ TJ BD TG TS YF CZ LC YC XL
BJ TJ BD TG TS YF CZ LC YC XL

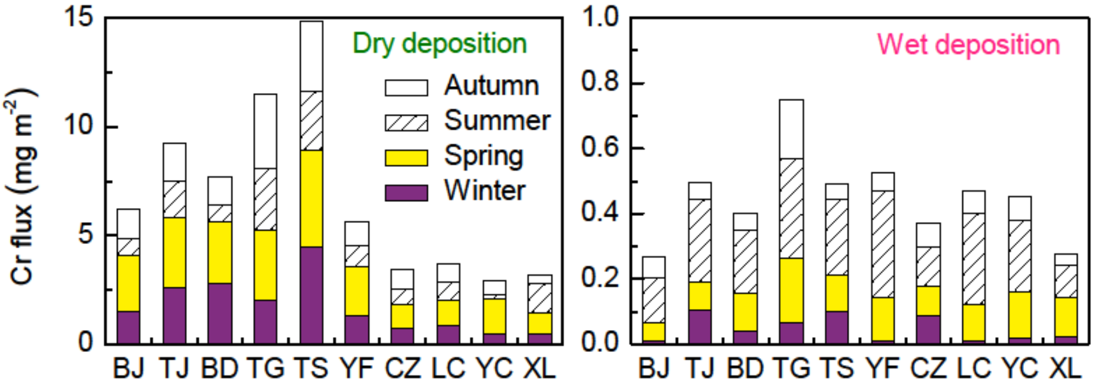
Cr flux (mg m^{-2})
Dry deposition
Autumn
Summer
Spring
Winter
Wet deposition
0
5
10
15
0.0
0.2
0.4
0.6
0.8
1.0
BJ TJ BD TG TS YF CZ LC YC XL
BJ TJ BD TG TS YF CZ LC YC XL

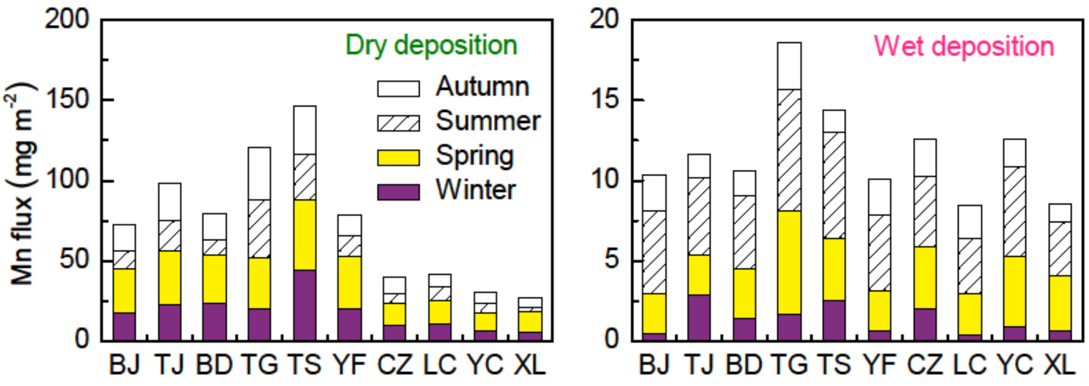
Mn flux (mg m^{-2})
Dry deposition
Autumn
Summer
Spring
Winter
Wet deposition
0
50
100
150
200
0
5
10
15
20
BJ TJ BD TG TS YF CZ LC YC XL
BJ TJ BD TG TS YF CZ LC YC XL

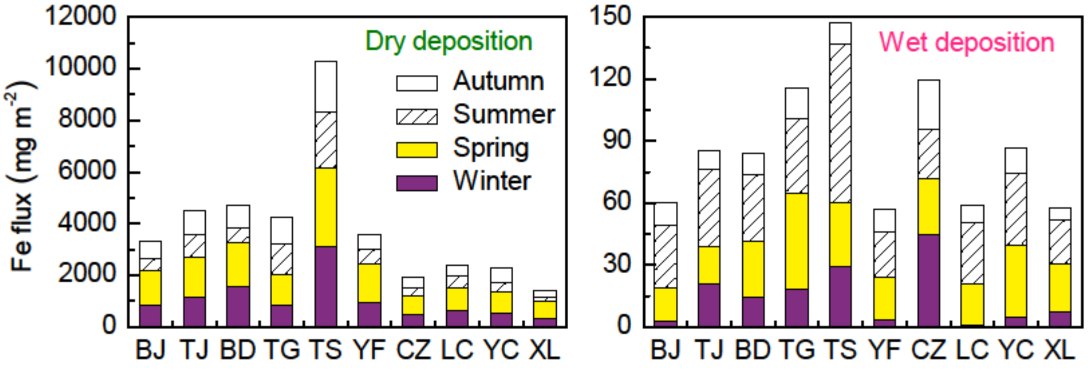
Fe flux (mg m^{-2})
Dry deposition
Autumn
Summer
Spring
Winter
Wet deposition
0
2000
4000
6000
8000
10000
12000
0
30
60
90
120
150
BJ TJ BD TG TS YF CZ LC YC XL
BJ TJ BD TG TS YF CZ LC YC XL

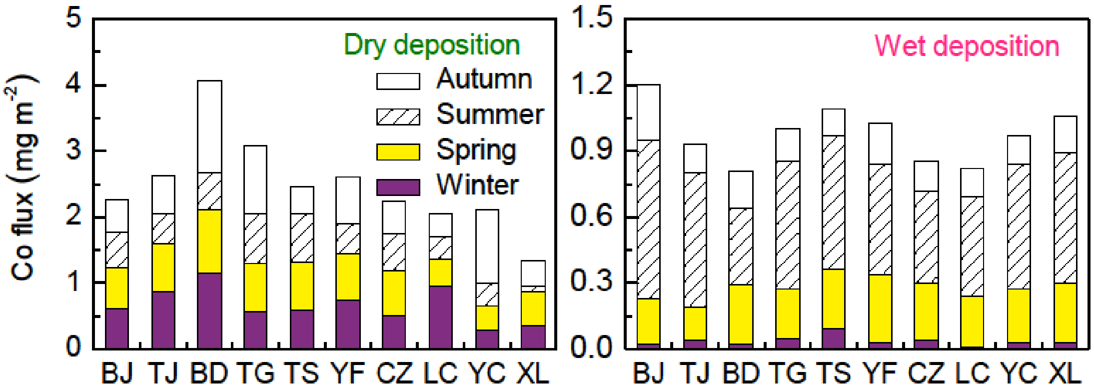
Co flux (mg m^{-2})
Dry deposition
Autumn
Summer
Spring
Winter
Wet deposition
0
1
2
3
4
5
0.0
0.3
0.6
0.9
1.2
1.5
BJ TJ BD TG TS YF CZ LC YC XL
BJ TJ BD TG TS YF CZ LC YC XL

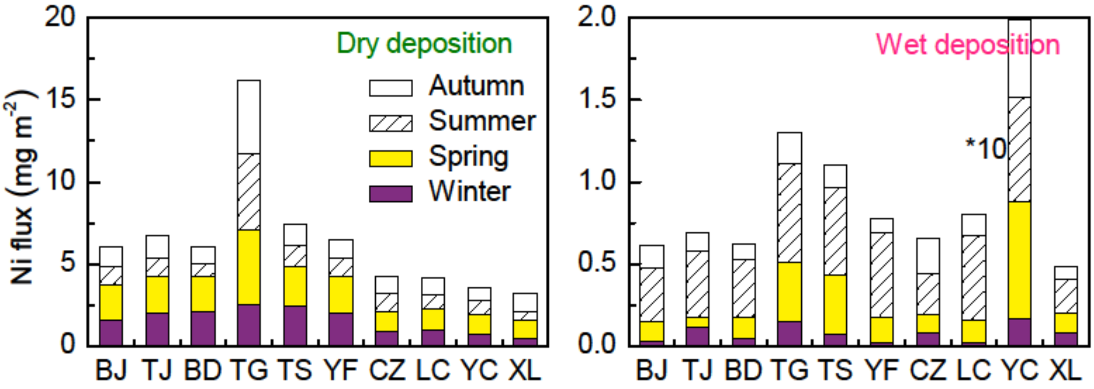
Ni flux (mg m^{-2})
Dry deposition
Autumn
Summer
Spring
Winter
Wet deposition
*10
0
5
10
15
20
0.0
0.5
1.0
1.5
2.0
BJ TJ BD TG TS YF CZ LC YC XL
BJ TJ BD TG TS YF CZ LC YC XL

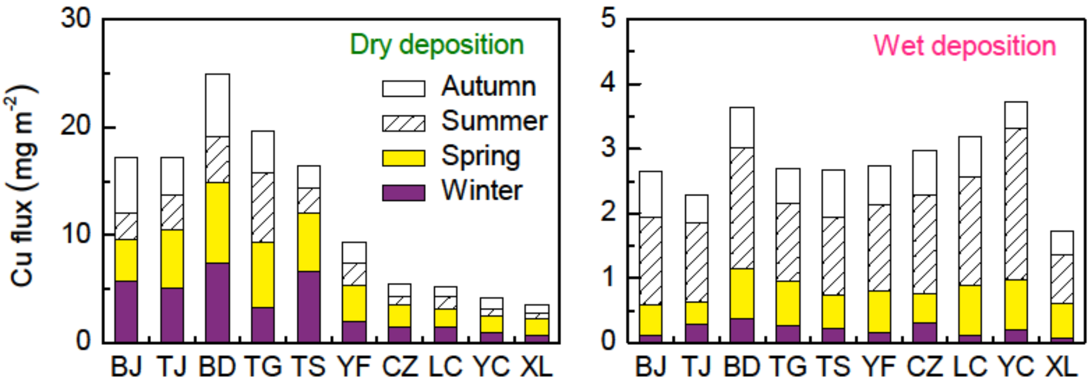
Cu flux (mg m^{-2})
Dry deposition
Autumn
Summer
Spring
Winter
Wet deposition
0
10
20
30
0
1
2
3
4
5
BJ TJ BD TG TS YF CZ LC YC XL
BJ TJ BD TG TS YF CZ LC YC XL

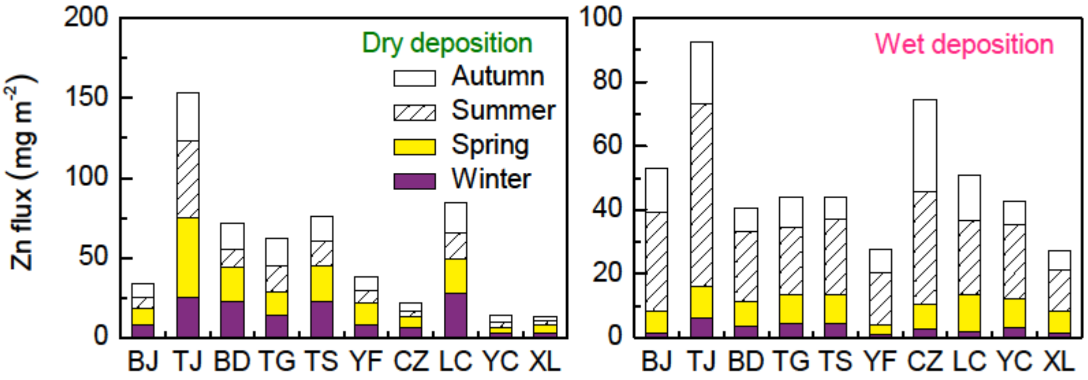
Zn flux (mg m^{-2})
Dry deposition
Autumn
Summer
Spring
Winter
Wet deposition
0
50
100
150
200
0
20
40
60
80
100
BJ TJ BD TG TS YF CZ LC YC XL
BJ TJ BD TG TS YF CZ LC YC XL

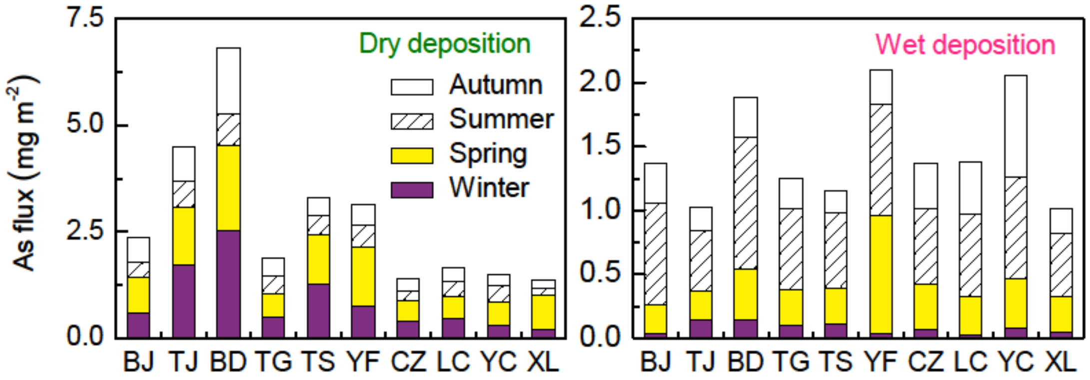
As flux (mg m^{-2})
7.5
5.0
2.5
0.0
Dry deposition
Autumn
Summer
Spring
Winter
BJ TJ BD TG TS YF CZ LC YC XL
2.5
2.0
1.5
1.0
0.5
0.0
Wet deposition
BJ TJ BD TG TS YF CZ LC YC XL

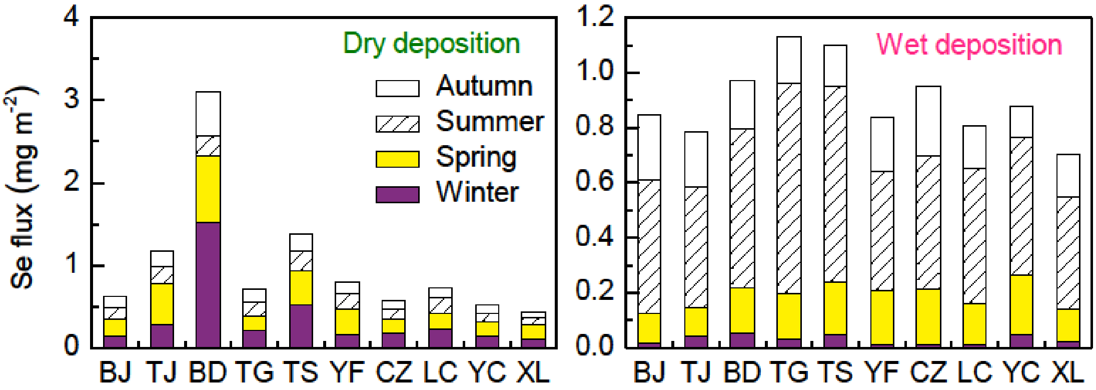
Se flux (mg m^{-2})
4
3
2
1
0
Dry deposition
Autumn
Summer
Spring
Winter
BJ TJ BD TG TS YF CZ LC YC XL
1.2
1.0
0.8
0.6
0.4
0.2
0.0
Wet deposition
BJ TJ BD TG TS YF CZ LC YC XL

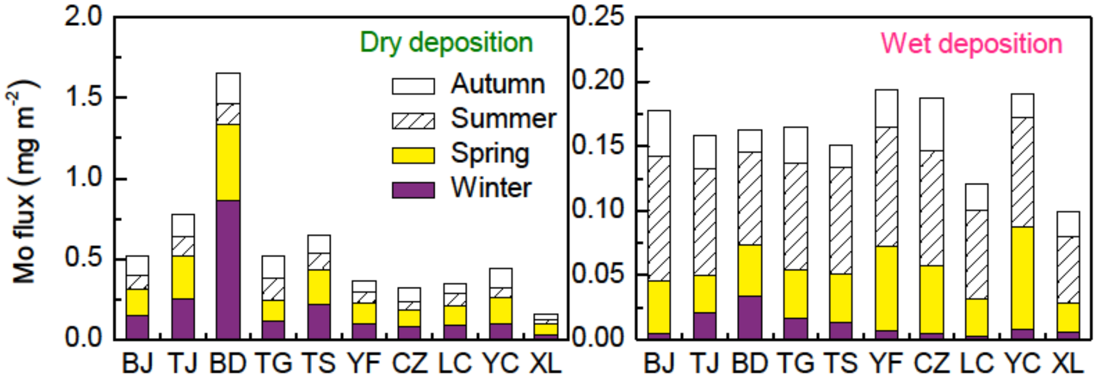
Mo flux (mg m^{-2})
2.0
1.5
1.0
0.5
0.0
Dry deposition
Autumn
Summer
Spring
Winter
BJ TJ BD TG TS YF CZ LC YC XL
0.25
0.20
0.15
0.10
0.05
0.00
Wet deposition
BJ TJ BD TG TS YF CZ LC YC XL

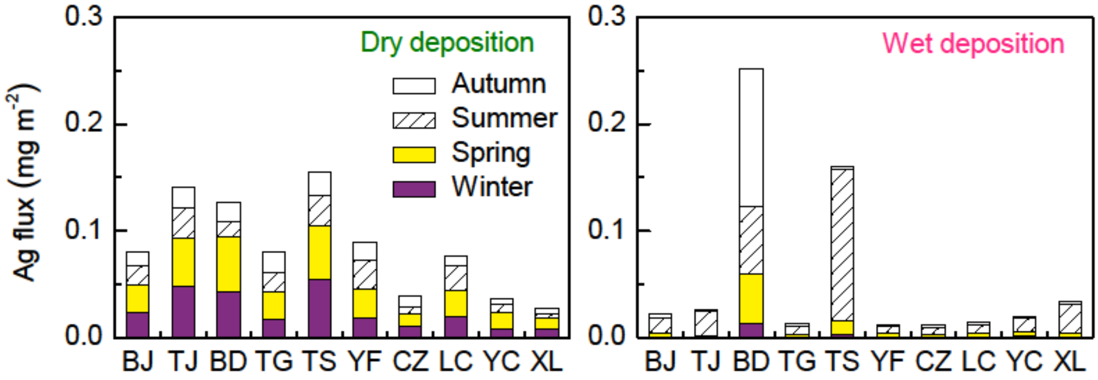
Ag flux (mg m^{-2})
0.3
0.2
0.1
0.0
Dry deposition
Autumn
Summer
Spring
Winter
BJ TJ BD TG TS YF CZ LC YC XL
0.3
0.2
0.1
0.0
Wet deposition
BJ TJ BD TG TS YF CZ LC YC XL

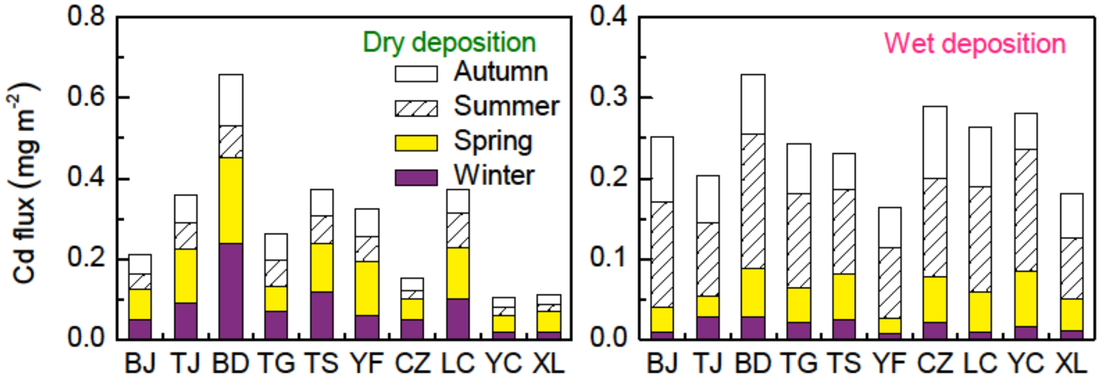
Cd flux (mg m^{-2})
Dry deposition
Autumn
Summer
Spring
Winter
Wet deposition
0.0
0.2
0.4
0.6
0.8
0.0
0.1
0.2
0.3
0.4
BJ TJ BD TG TS YF CZ LC YC XL
BJ TJ BD TG TS YF CZ LC YC XL

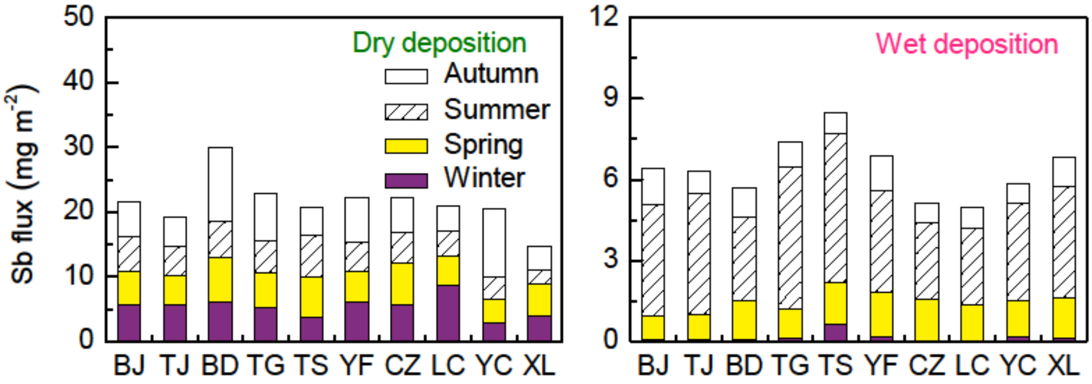
Sb flux (mg m^{-2})
Dry deposition
Autumn
Summer
Spring
Winter
Wet deposition
0
10
20
30
40
50
0
3
6
9
12
BJ TJ BD TG TS YF CZ LC YC XL
BJ TJ BD TG TS YF CZ LC YC XL

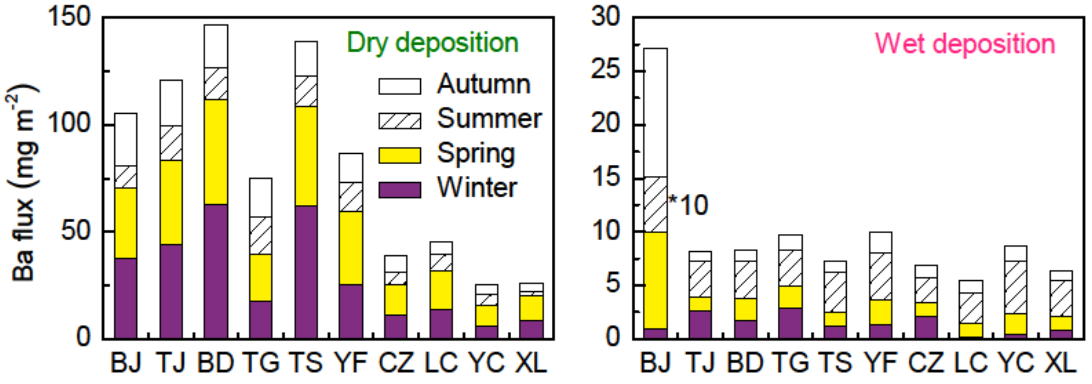
Ba flux (mg m^{-2})
Dry deposition
Autumn
Summer
Spring
Winter
Wet deposition
*10
0
50
100
150
0
5
10
15
20
25
30
BJ TJ BD TG TS YF CZ LC YC XL
BJ TJ BD TG TS YF CZ LC YC XL

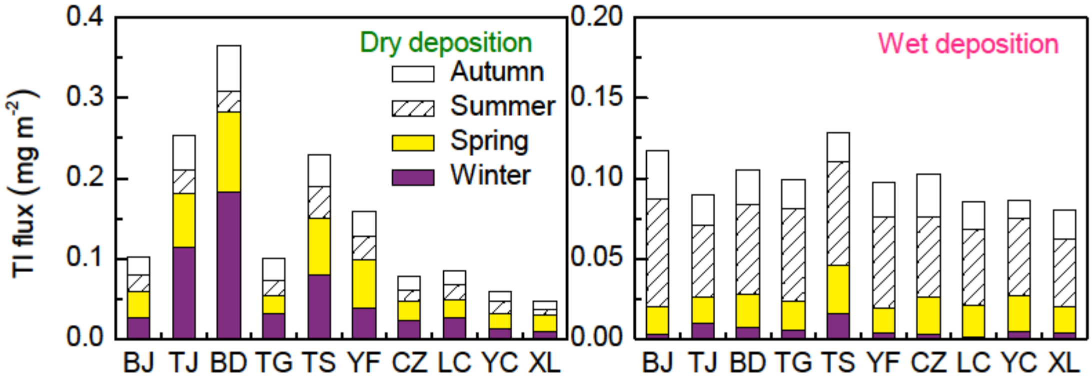
Tl flux (mg m^{-2})
Dry deposition
Autumn
Summer
Spring
Winter
Wet deposition
0.0
0.1
0.2
0.3
0.4
0.00
0.05
0.10
0.15
0.20
BJ TJ BD TG TS YF CZ LC YC XL
BJ TJ BD TG TS YF CZ LC YC XL

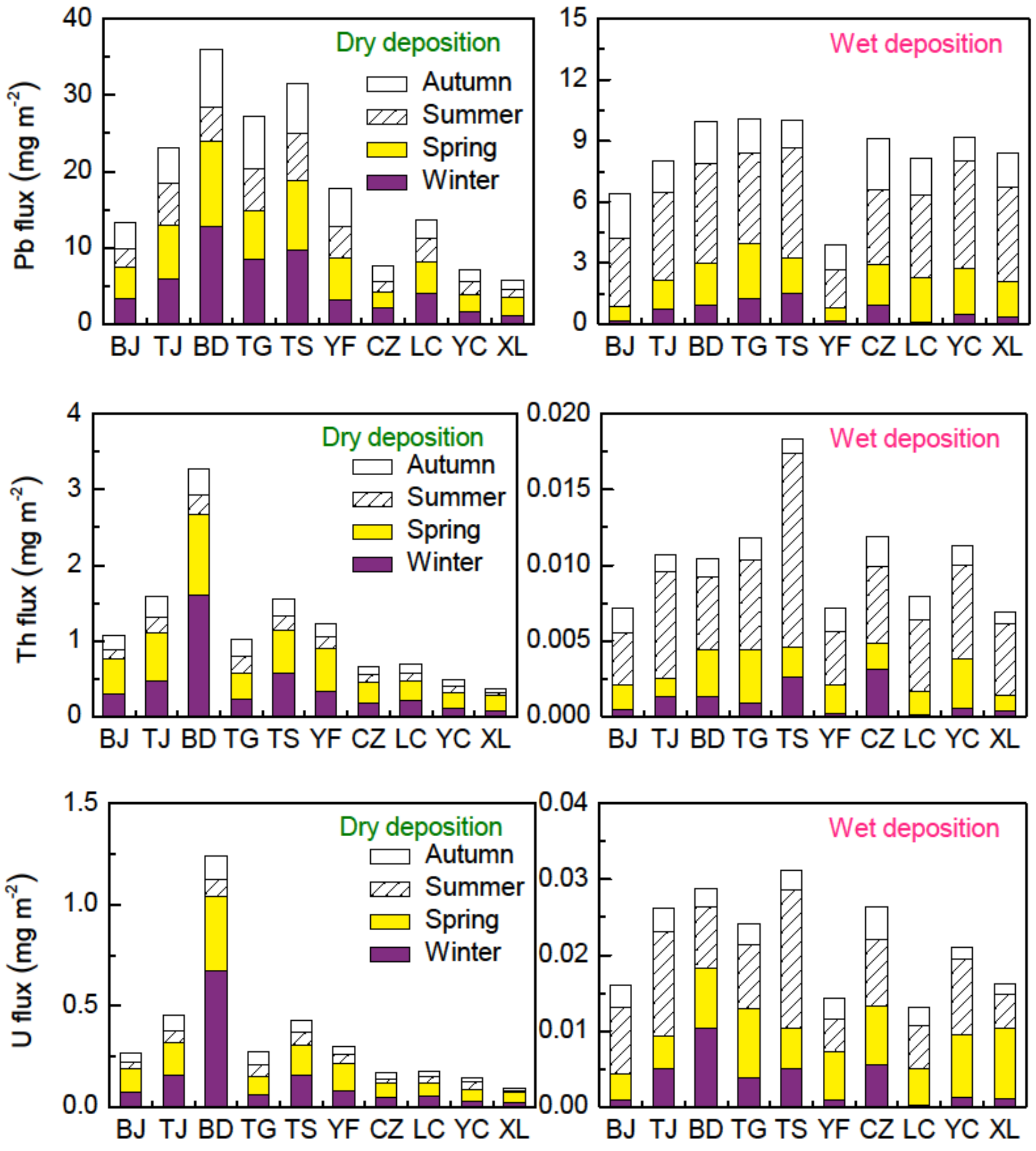

Fig. 3. Spatial distribution and seasonal variations in atmospheric wet and dry deposition fluxes of trace elements in Northern China.

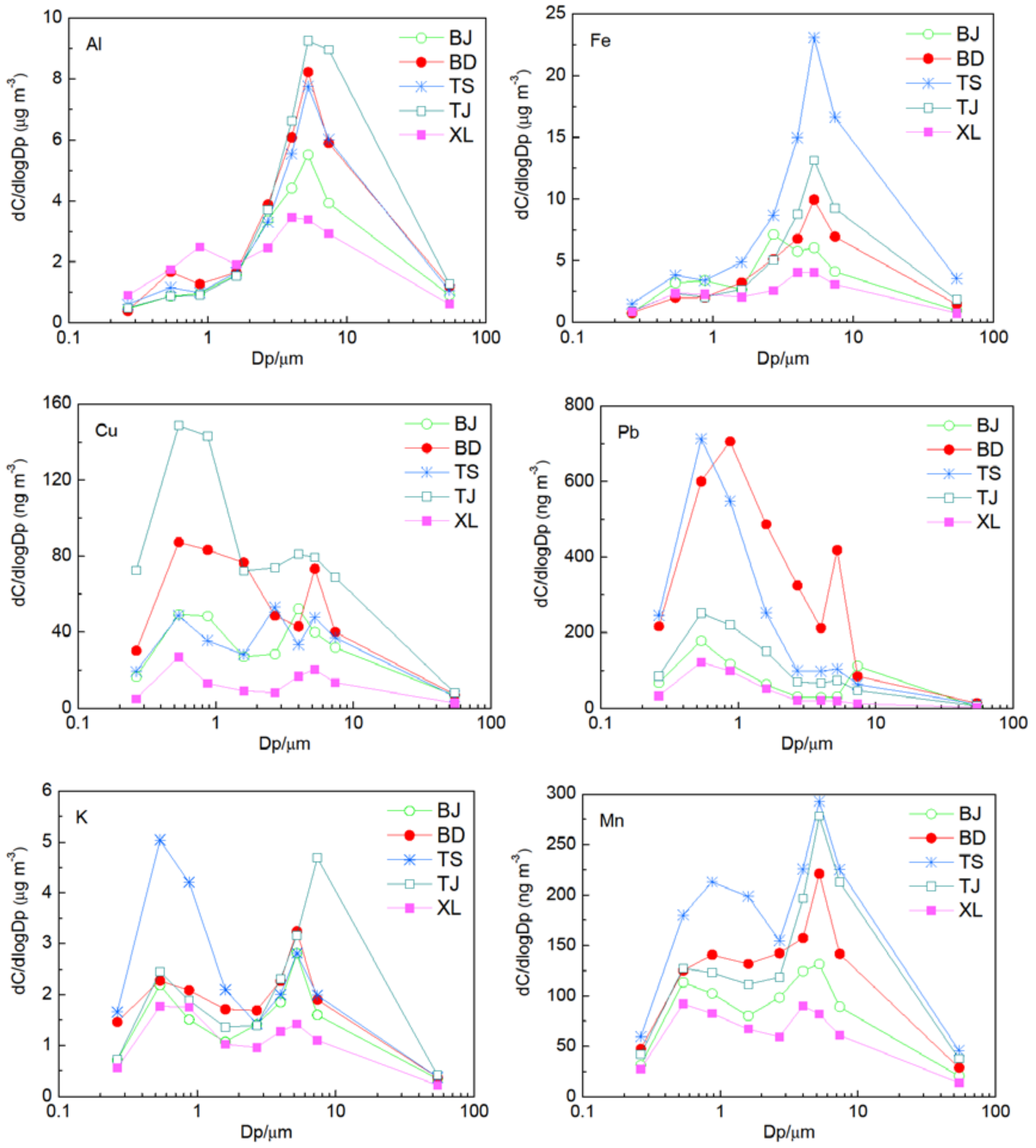

Fig. 4. Size distribution of aerosol trace elements in Northern China.

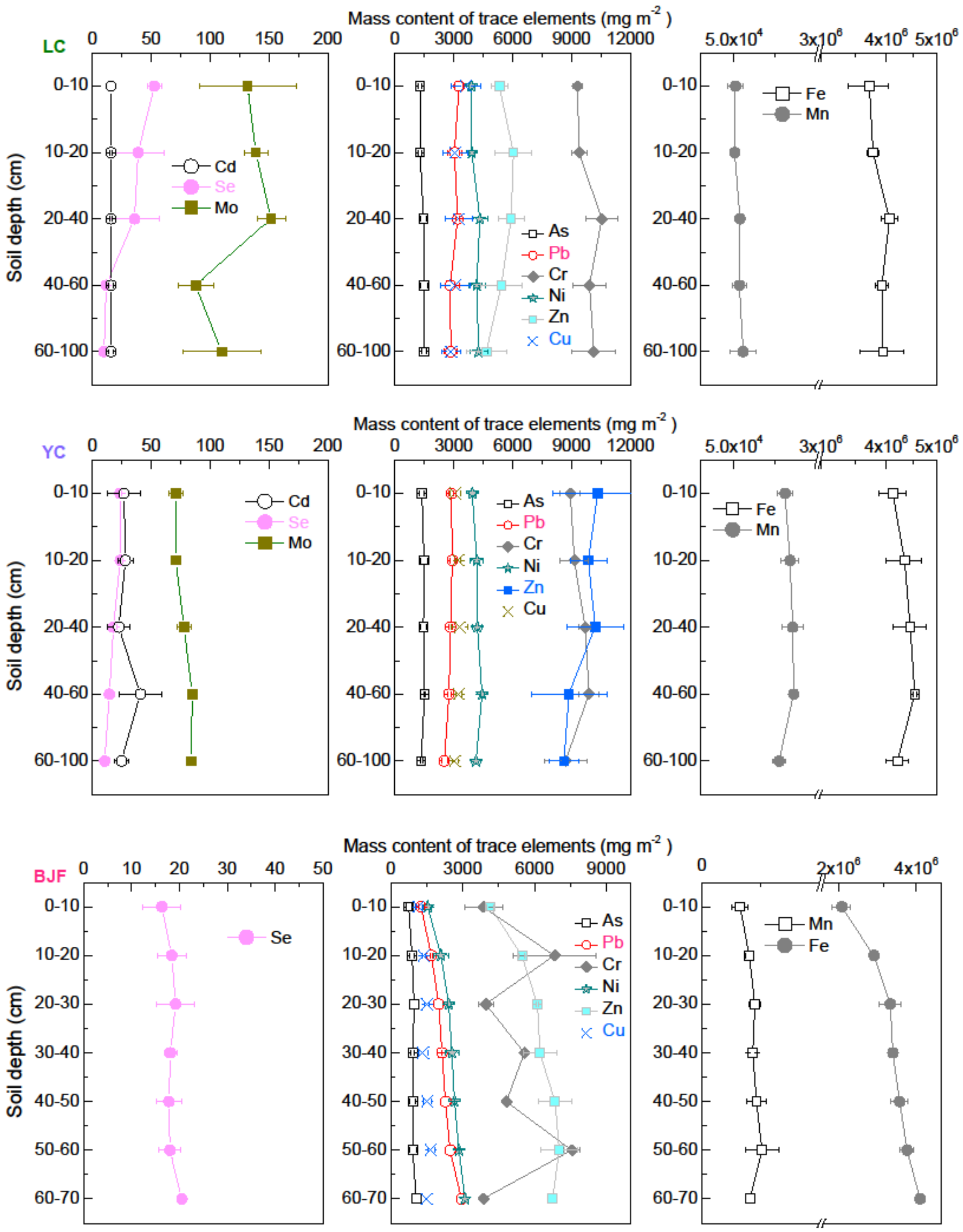

Fig. 5. Soil profile of selected elements from three typical agricultural and forest sites in Northern China.